

Nonlocal Finite-Depth Circuits for Constructing Symmetry-Protected Topological States and Quantum Cellular Automata

David T. Stephen^{1,2,*}, Arpit Dua^{2,†}, Ali Lavasani³ and Rahul Nandkishore¹

¹*Department of Physics and Center for Theory of Quantum Matter, University of Colorado Boulder, Boulder, Colorado 80309, USA*

²*Department of Physics, California Institute of Technology, Pasadena, California 91125, USA*

³*Kavli Institute for Theoretical Physics, University of California, Santa Barbara, Santa Barbara California 93106, USA*



(Received 10 January 2023; accepted 20 December 2023; published 11 January 2024)

Whether a given target state can be prepared by starting with a simple product state and acting with a finite-depth quantum circuit is a key question in condensed matter physics and quantum information science. It underpins classifications of topological phases, as well as the understanding of topological quantum codes, and has obvious relevance for device implementations. Traditionally, this question assumes that the quantum circuit is made up of unitary gates that are *geometrically local*. Inspired by the advent of noisy intermediate-scale quantum devices, we reconsider this question with *k-local* gates, i.e., gates that act on no more than k degrees of freedom but are not restricted to be geometrically local. First, we construct explicit finite-depth circuits of symmetric k -local gates that create symmetry-protected topological (SPT) states from an initial product state. Our construction applies to SPT states protected by global symmetries or subsystem symmetries but not to those with higher-form symmetries, which we conjecture remain nontrivial. Next, we show how to implement arbitrary translationally invariant quantum cellular automata in any dimension using finite-depth circuits of k -local gates. These results imply that the topological classifications of SPT phases and quantum cellular automata both collapse to a single trivial phase in the presence of k -local interactions. We furthermore argue that SPT phases are fragile to *generic* k -local symmetric perturbations. We conclude by discussing the implications for other phases, such as fracton phases, and surveying future directions. Our analysis opens a new experimentally motivated conceptual direction examining the stability of phases and the feasibility of state preparation without the assumption of geometric locality.

DOI: [10.1103/PRXQuantum.5.010304](https://doi.org/10.1103/PRXQuantum.5.010304)

I. INTRODUCTION

The exploration of *topological phases of matter* has been a major theme of modern condensed matter physics (for introductions, see Refs. [1,2]), with far-reaching implications for quantum information and quantum computation (for introductions, see Refs. [3,4]). These phases of matter, when defined on lattices, have been classified with use of the complexity of preparation of the associated ground states using local quantum circuits (QCs) [5]; a state that can be accessed by starting with a product state

and acting with a finite-depth quantum circuit (FDQC) of geometrically local gates can be said to be “easy” to prepare, and one that cannot be is difficult to prepare. This characterization is intimately related to the notion of *topological stability*, which states that topological phases are robust to geometrically local perturbations [which should be symmetry restricted in the case of symmetry-protected topological (SPT) phases [6,7]], since topological stability implies that topologically nontrivial states cannot be connected to trivial states by a (symmetric) FDQC [5,8]. Recently, the notion of FDQCs in relation to topological phases has been extended in various directions, such as allowing projective measurements [9–11], or by extension to linear-depth quantum circuits [12–14], but still demanding geometric locality. The geometric locality is, of course, a very natural constraint to impose in traditional solid-state settings. However, we are witnessing the rapid development of experimental capabilities in the fields of quantum simulation and noisy intermediate-scale quantum devices

*davidtstephen@gmail.com

†adua@caltech.edu

Published by the American Physical Society under the terms of the [Creative Commons Attribution 4.0 International](https://creativecommons.org/licenses/by/4.0/) license. Further distribution of this work must maintain attribution to the author(s) and the published article's title, journal citation, and DOI.

(for a recent review, see Ref. [15]), which have come to provide a new context in which to explore topological phases (see e.g., Refs. [16,17]). In this new setting, the geometric locality is not necessarily guaranteed and there can arise k -local interactions, i.e., interactions involving few bodies (acting on no more than k degrees of freedom) but not restricted to be geometrically local (see e.g., Refs. [18–21]). Do the results on the difficulty of topological state preparation survive in this new setting, and does the classification of topological phases of matter and the associated notion of topological stability survive in a setting where there can be k -local perturbations?

Another topological classification that may be affected by k -local interactions is that of locality-preserving unitary operators, also known as quantum cellular automata (QCA) [22]. An FDQC is an obvious example of a QCA, but there are also QCA that cannot be written as an FDQC, such as the lattice translation operator. The topological classification of phases of QCA arises from the question of whether two QCA can be smoothly connected along a locality-preserving path, with the topologically trivial phase consisting of FDQCs as they can be connected to the identity. In one and two dimensions, this classification is given by an index theory that essentially shows that every QCA can be decomposed as an FDQC and a translation [23,24]. In three dimensions, the classification is incomplete as there appear to be QCA that are neither FDQCs nor translations, but significant progress is being made [25–27]. The classification of QCA also plays a role in the classification of topological phases [25–29], particularly Floquet phases [30–32].

In this work, we examine the fate of the “topological stability” of topological phases and QCA in the presence of k -local perturbations by asking whether one can construct a reference state or QCA in the putatively topological phase using an FDQC made out of k -local (but not geometrically local) gates. We show that SPT phases with global or subsystem symmetries are *not* stable to k -local perturbations by explicitly constructing FDQCs of symmetric k -local gates that trivialize the fixed-point states by mapping them to symmetric product states. Since all states within a given phase can be connected to the fixed-point state by a symmetric FDQC [5], our circuits for fixed-point states imply the existence of similar circuits that disentangle any state in a given SPT phase. We also argue that SPT order should be unstable to generic symmetric k -local noise. Similarly, we show that every translationally invariant QCA on a periodic lattice in any spatial dimension can be realized as an FDQC of k -local gates that commute with the same symmetries as the QCA. Therefore, all QCA belong to the same trivial phase when k -local gates are allowed. However, k -local perturbations do not trivialize everything—indeed it is known that topological order (such as the toric code model) is stable to k -local perturbations [33]. More generally, it is known that code states of

quantum error correcting codes cannot be disentangled in finite depth by k -local unitary gates [8,33] (see Appendix D for a brief review of the proof). We argue that fracton order and Floquet topological codes are also stable to k -local perturbations, and we conjecture the same is true of SPT order protected by higher-form symmetries.

While our main focus is on “in principle” topological classifications in the absence of geometric locality, our work also has practical implications. In particular, we note that there has recently been a significant effort to prepare and analyze topological phases in quantum simulators and quantum computers [34–40]. In this context, our results show that certain operations that require a circuit depth that is linear in system size with local interactions can be done in finite depth using k -local interactions, significantly reducing the time required for implementation.

In summary, this paper introduces a new (experimentally motivated) perspective on topological stability, showing that certain topological classifications can collapse in the presence of k -local interactions, and also opens up a new route for the efficient preparation of certain topological states on quantum devices.

The rest of this paper is organized as follows. In Sec. II we provide a precise definition of k -local circuits. In Sec. III we show that these circuits can trivialize arbitrary SPTs protected by global or subsystem symmetries, but we provide evidence that this is not possible for SPTs protected by higher-form symmetries. In Sec. IV we show that these circuits can also trivialize arbitrary QCA. In Sec. V A we present numerical evidence that such circuits can trivialize SPT states in monitored circuits. We conclude in Sec. VI, where we also discuss the k -local nontriviality of states with true topological order (including fracton phases and Floquet topological codes) and the implications of our results and some future directions. In Appendix A, we discuss an alternative classification based on *finite-time* k -local circuits, which are even more powerful than the finite-depth k -local circuits discussed in the main text.

II. DEFINITION OF k -LOCAL CIRCUITS

In this section, we lay out the definitions of the notions of locality that we are concerned with throughout the paper. The first and most common notion of locality is geometric locality. Any lattice system has a natural notion of distance between pairs of sites, which allows us to define a geometrically local unitary gate as one that acts only on sites that can be contained within a ball of some finite radius. Here and throughout this paper, the word “finite” means independent of system size, i.e., finite even in the thermodynamic limit. Naturally, such a gate acts only on a finite number of sites in the lattice. One can construct a

circuit of geometrically local gates

$$U = \prod_{\ell=1}^D \left(\prod_i u_{\ell,i} \right) \quad (1)$$

where each gate $u_{\ell,i}$ is geometrically local and the gates within a given layer ℓ have nonoverlapping support, such that they can be applied in parallel. We call such a unitary U a QC. When the number of layers D is finite, U is called an FDQC. It is also interesting to define symmetric QCs, which are circuits in which each gate individually commutes with some symmetry operator.

We can extend the notion of the geometric locality to k locality. A gate is called “ k local” if it has support on at most k sites. Thus, a k -local gate shares the few-body property of a geometrically local gate while ignoring the relative position and distance between spins. We define a k -local quantum circuit, QC_k , to be composed of k -local gates $u_{\ell,i}$, where k is finite, such that the gates are applied in layers and in each layer they have nonoverlapping support. When the number of layers is finite, we call the circuit a finite-depth QC_k (FDQC $_k$).

Clearly, every QC is also a QC_k , but in general, a QC_k is more powerful in the sense that writing a many-body unitary operator as a QC_k can sometimes be accomplished with lower depth than is required to write it as a QC. As a simple example, consider the unitary operator that generates the N -qubit Greenberger-Horne-Zeilinger (GHZ) state from a product state. This can be implemented only with a linear-depth QC due to the presence of long-range correlations in the GHZ state [33]. However, it can be done with a QC_k having a depth that is logarithmic in N ; see Refs. [41,42], for example. Similarly, the unitary that generates the 2D toric code ground state, an example of topological order, requires a linear-depth QC [8] but can be done in a log-depth QC_k [42,43]. Notably, neither of these unitaries can be written as an FDQC $_k$ [33], so we say that the GHZ and toric code states remain nontrivial in the k -local setting. In contrast, the unitaries discussed in this paper will primarily be circuits that require linear depth with use of a (symmetric) QC, but can be performed in finite depth with use of a (symmetric) QC_k , so we say they become trivial in the k -local setting.

III. k -LOCAL INSTABILITY OF SPTs

In this section, we ask whether SPT states can be prepared by a symmetric FDQC $_k$. In Secs. III A and III B we consider global on-site symmetries. While it is known that a linear-depth symmetric QC is needed to create an SPT ground state [12] from a symmetric product state, we show that a symmetric FDQC $_k$ is sufficient. We first give an intuitive physical argument as to why this is the case by studying the boundaries of SPT phases, and we then construct an explicit finite-depth k -local symmetric circuit that

disentangles fixed-point SPT states. In Sec. III C, we show that SPT phases protected by subsystem symmetries (SSPT phases) can also become trivial in the k -local scenario. Conversely, we argue in Sec. III D that SPT phases protected by higher-form symmetries remain nontrivial even in the k -local scenario. In Appendix A, we give alternative finite-time k -local constructions of SPT states that have the advantage that all interactions are local except for one special qubit that can interact with all other qubits.

A. One-dimensional SPT phases with global symmetries

We first consider 1D SPT phases. The characteristic feature of 1D SPT order is the existence of zero-energy edge modes that are protected by the bulk symmetry. On periodic boundaries, the ground state is unique. But when an edge is introduced, degenerate ground states that differ only in a region exponentially close to the boundary will appear. This boundary degeneracy is robust in the sense that no local, symmetric perturbation can split the degeneracy. However, the degeneracy is not robust to k -local interactions, as a symmetric interaction can be used to couple the two edges in such a way as to split the degeneracy. This suggests that 1D SPT orders are not robust to k -local symmetric interactions. However, there may still be some nontrivial bulk properties that cannot be removed by k -local interactions. We show that this is not the case by explicitly constructing a symmetric FDQC $_k$ that maps generic SPT fixed-point states to product states.

We can understand why such a circuit should exist using a simple folding argument. Namely, consider a 1D SPT ordered state $|\psi\rangle$ on a ring. Suppose that we “fold” the ring, bringing the two opposite sides close to each other. In the bulk of the folded system, it looks like we have stacked the state with its spatially reversed self; see Fig. 1. However, it is well known that SPT phases are invertible, meaning that there exists a second state $|\psi^{-1}\rangle$ such that the joint system $|\psi\rangle \otimes |\psi^{-1}\rangle$ is in a trivial SPT phase. For this statement to make sense, it is important to specify how the symmetry acts on the joint system. If $|\psi\rangle$ has symmetry G with an on-site representation $U(g)$, then the symmetry acts on the joint system “diagonally,” i.e., with representation $U(g) \otimes U(g)$ of G . If we instead considered the symmetry group $G \times G$ represented by $U(g) \otimes U(h)$ with g not necessarily equal to h , then the stacked system is still in a nontrivial phase with respect to this larger symmetry. In the folded system, the global symmetry indeed acts in the same way across the whole ring, so the total symmetry group is still only G .

It turns out that the spatial inverse of the SPT fixed-point states is in fact the inverse state in the above sense [7], so the bulk of the folded system looks like a trivial SPT phase. Then there must be a symmetric finite-depth circuit that disentangles the bulk to a product state. Looking at

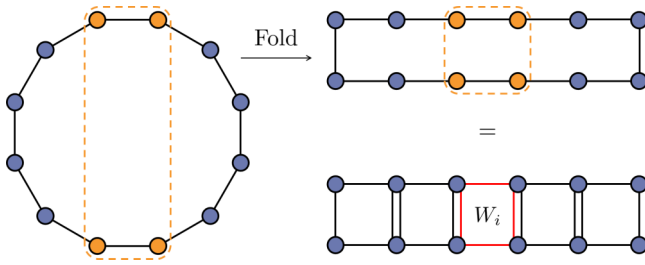


FIG. 1. Disentangling 1D SPT phases with k -local symmetric gates. After the folding of a 1D chain with periodic boundary conditions in half, the resulting system looks like a stack of the chain and its spatial inverse in the bulk. This stack can be disentangled with symmetric gates acting on the highlighted qubits, which correspond to k -local gates in the original system. For fixed-point SPT states, these gates are the W_i defined in Eq. (3); one such gate is highlighted in red, where each line is a CZ gate. Note that the adjacent vertical gates cancel each other pairwise in the bulk.

this picture without folding, we see that the disentangling circuit couples the two distant edges of the ring, therefore requiring long-range k -local gates.

Let us explicitly construct such a circuit. We give only a single example here, as the general case is covered by the construction in Sec. IV. The example we consider is the 1D cluster state [44], which can be created from a product state with use of a finite circuit in the following way:

$$|\psi_C\rangle = \left(\prod_{i=1}^N \text{CZ}_{i,i+1} \right) |+\rangle^{\otimes N}, \quad (2)$$

where $|+\rangle = \frac{1}{\sqrt{2}}(|0\rangle + |1\rangle)$ and $\text{CZ} = I - 2|11\rangle\langle 11|$ is the controlled- Z gate. Assuming N is even, $|\psi_C\rangle$ has a $\mathbb{Z}_2 \times \mathbb{Z}_2$ symmetry generated by $X_{\text{odd}} = \prod_{i=1}^{N/2} X_{2i+1}$ and $X_{\text{even}} = \prod_{i=1}^{N/2} X_{2i}$.

Importantly, while the circuit of controlled- Z gates commutes with this symmetry as a whole, the individual gates do not. Since the 1D cluster state has nontrivial SPT order [45], there does not exist a symmetric FDQC that maps it to a product state [12,46]. However, mapping is possible with use of a symmetric FDQC_k . Consider the gates

$$W_i = \text{CZ}_{i,i+1} \text{CZ}_{i+1,N-i} \text{CZ}_{N-i,N-i+1} \text{CZ}_{N-i+1,i}, \quad (3)$$

which are depicted in Fig. 1. It is straightforward to check that W_i commutes with the $\mathbb{Z}_2 \times \mathbb{Z}_2$ symmetry. Furthermore, we have,

$$\left(\prod_{i=1}^{N/2-1} W_i \right) |\psi_C\rangle = |+\rangle^{\otimes N}, \quad (4)$$

as shown in Fig. 1. Since the W_i all commute with each other, and since the support of each W_i overlaps with the

support of finitely many others, they can be applied in a finite number of layers such that this is a symmetric FDQC_k that trivializes the cluster state.

It is instructive to note that W_i is the operator that creates a small four-site cluster state on a ring, which explains why it is symmetric. The k -local disentangling circuit can therefore be interpreted as a ‘‘bubbling’’ procedure in which one decomposes the N -site cluster state into a number of small four-site cluster states and then disentangles each four-site cluster state with a symmetric k -local gate.

B. Two-dimensional and higher-dimensional SPT phases

The folding argument from the previous section carries over equally well to SPT phases with global symmetries in two dimensions and higher. We give only the 2D argument explicitly, as the generalization to higher dimensions is straightforward. We again give a single example as the general case (in all dimensions) is covered in Sec. IV.

As in one dimension, we can predict that 2D SPT phases are trivial with k -local interactions by considering the boundary. Consider the example of a topological insulator, which has a gapless helical edge on the boundary of a disk. With local symmetric interactions, the edge cannot be gapped out without breaking the symmetry (although see Refs. [47,48]). However, two opposite points on the boundary have helical currents moving in opposite directions, which could backscatter off each other if coupled by a k -local perturbation. Therefore, it is possible to introduce a k -local symmetric term that couples opposite points and gaps out the edge without breaking symmetry.

As before, we confirm this intuition by constructing explicit symmetric FDQC_k disentanglers. As our example, we choose the 2D hypergraph state, first defined in Ref. [49]. The state is defined on a triangular lattice with one qubit per site. We choose boundary conditions of a sphere for our demonstration, but a torus would work equally well. The state is defined as follows:

$$|\psi_H\rangle = \left(\prod_{\Delta} \text{CCZ}_{\Delta} \right) |+\rangle^{\otimes N} \quad (5)$$

where the controlled-controlled- Z (CCZ) gate acts on the three qubits around a triangle as $\text{CCZ} = I - 2|111\rangle\langle 111|$. This state has SPT order protected by a $\mathbb{Z}_2 \times \mathbb{Z}_2 \times \mathbb{Z}_2$ symmetry [49]. This symmetry relies on the fact that the lattice is three colorable, meaning that each site can be assigned a color (red, blue, or green) such that neighboring sites have different colors; see Fig. 2. The symmetry is then generated by the operators $X_R, X_B,$ and X_G , which are tensor products of X on every red, blue, and green site, respectively. This state is closely related to the Levin-Gu state [50], which is an example of 2D SPT order with \mathbb{Z}_2

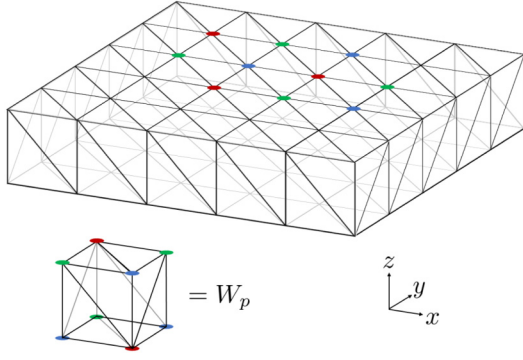


FIG. 2. Disentangling 2D SPT phases with k -local symmetric gates. We show a folded system with spherical boundary conditions, which leads to a thin rectangular prism. A torus is obtained by identification of the left and right faces. A subset of the lattice coloring is shown. The rectangular prism geometry can be decomposed into smaller rectangular prisms. The symmetric gate W_p is defined by our acting with a CCZ gate on all 12 triangular faces of this prism. When W_p is applied to every prism, all bulk gates that act on faces parallel to the z axis cancel between neighboring prisms, leaving only gates on the surface of the large rectangular prism.

symmetry [51]. As before, the circuit of CCZ gates is symmetric as a whole on closed boundary conditions, but the individual gates are not symmetric.

By folding the 2D system, we get a state defined on the surface of a thin rectangular prism. This rectangular prism can be decomposed into a number of small rectangular prisms with triangular faces; see Fig. 2. We label these prisms by $p \in P$. For each such prism p , we define a gate

$$W_p = \prod_{\Delta \in p} \text{CCZ}_{\Delta}, \quad (6)$$

which is depicted in Fig. 2. As in the 1D case, this operator can be interpreted as creating a small instance of $|\psi_H\rangle$ on a triangulation of a sphere, and it, therefore, respects the $\mathbb{Z}_2 \times \mathbb{Z}_2 \times \mathbb{Z}_2$ symmetry. Applying this operator to every prism, we have

$$\left(\prod_{p \in P} W_p \right) |\psi_H\rangle = |+\rangle^{\otimes N}, \quad (7)$$

so this is a symmetric FDQC_k disentangler.

C. SPT phases with subsystem symmetries

We now turn to SPT phases protected by subsystem symmetries. These are symmetries that act on rigid, lower-dimensional submanifolds of the entire system, such as straight lines across a 2D lattice [52–56]. These are similar to 1D SPTs, in that they are characterized by an extensive degeneracy on the edge [53,54]. Indeed, if a 2D SSPT

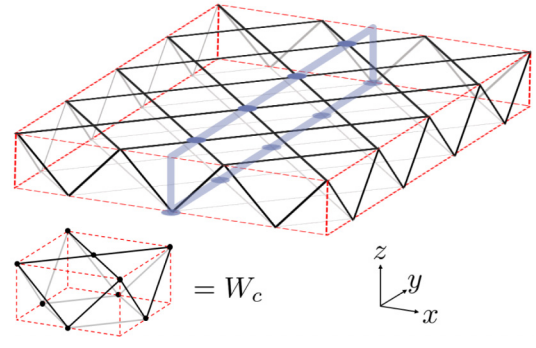


FIG. 3. Disentangling 2D SSPT phases with k -local symmetric gates. The dashed lines are shown as a guide for the eye. A torus is obtained by identification of the left and right opposite faces. The gate W_c consists of CZ operations on every solid edge, with qubits located at the small dots (not drawn in the upper figure). The thick solid loop and dots indicate the support of one linelike subsystem symmetry generator.

phase on a cylinder is treated like a quasi-1D system along the cylinder's length, then it behaves like a 1D SPT phase with a subextensive number of symmetry generators [28].

The prototypical SSPT phase is represented by the 2D cluster state [44]. This state consists of qubits on a 2D square lattice and is defined as follows:

$$|\psi_{2DC}\rangle = \left(\prod_{\langle ij \rangle} \text{CZ}_{ij} \right) |+\rangle^{\otimes N}, \quad (8)$$

where the product is over all nearest neighbors in the square lattice. The symmetries of this model form rigid diagonal lines spanning the square lattice, defined as

$$U_{c,\pm} = \prod_x X_{(x,c\pm x)}, \quad (9)$$

where $i = (x, y)$ is a coordinate on the 2D square lattice. Similarly to the cases of global symmetry, one can use the folding trick to create $|\psi_{2DC}\rangle$ on a closed 2D manifold using a symmetric FDQC_k consisting of the symmetric k -local gates W_c defined in Fig. 3.

For a diagonal line of symmetry to act the same on the top and bottom layers of the fold as in Fig. 3—which is necessary for the folding argument to work—we needed to put $|\psi_{2DC}\rangle$ on a 45°-rotated square lattice. This results in some triangular faces appearing on spherical boundaries (which are absent on the torus). For general subsystem symmetries, which can have more complex geometries such as fractal geometries [55], we expect that a symmetric FDQC_k will be able to create SSPT states only on spatial manifolds with nice enough geometry such that there are distant regions in space where the symmetry mirrors itself.

D. SPT phases with higher-form symmetries

In this section, we argue that in contrast to phases protected by global and subsystem symmetries, phases protected by higher-form symmetries are robust to k -local symmetric interactions. In general, a q -form symmetry is one that acts on closed codimension- q submanifolds of space. In contrast to subsystem symmetries, these submanifolds are not rigid and can be deformed freely. These symmetries are local in the sense that they may have support on only a finite number of sites. For example, a one-form symmetry in three dimensions is generated by objects acting on any closed 2D surface embedded in the 3D space. A simple example of a state with SPT order under higher-form symmetries is the 3D cluster state defined in Ref. [57] (see also Ref. [58] for a more detailed discussion of the SPT order), which is also an example of the general Walker-Wang construction [59].

We first observe that the folding argument used for global symmetries does not carry over to the case of higher-form symmetries. This is because folding in this case does not correspond to stacking in the usual sense. Recall that stacking requires the symmetry to act in the same way on the two layers. When we fold a system with global symmetry, acting with the symmetry on the whole system automatically has identical action on the two layers of the fold. However, this is not the case when we fold a system with higher-form symmetry, since the symmetry generators, being local, can act independently on either layer. Because of this, the bulk of the folded system resembles two stacked SPT states, each with their own independent symmetry, and such a system has nontrivial SPT order.

Second, we observe that any k -local interaction that commutes with a higher-form symmetry is also locally symmetric, meaning the gates can be decomposed into a sum of tensor products of geometrically local symmetric unitaries. This is due to the simple fact that the higher-form symmetry group itself contains operators that act nontrivially only in local regions of space. This is very different from the case of global symmetries, where a symmetric k -local interaction can violate symmetry locally while still preserving it globally. Because of this, the class of k -local gates that we can use is severely restricted compared with the case of global symmetry. Indeed, the FDQC_k s used to disentangle the SPT states above commute only with the symmetry globally as they contain operators such as a long-range ZZ pair that can transfer symmetry charge over long distances. In Sec. V, we argue that the fact that symmetric k -local interactions can violate the symmetry in local regions of space is crucial to their ability to destroy SPT order. Accordingly, we expect that k -local gates that preserve the symmetry locally, which is always the case for higher-form symmetric gates, are not sufficient to destroy SPT order.

Finally, examination of the boundary of a higher-form SPT also suggests that it may be k -local nontrivial. Higher-form SPTs in three dimensions, for example, can support topologically ordered boundary theories such as a 2D toric code appearing on the boundary of the 3D cluster state [49,58,59]. However, unlike in the boundaries of systems with global symmetry discussed above, k -local interactions cannot trivialize this boundary theory because the 2D toric code, and any number of stacks of it, is k -local nontrivial [33].

IV. UNIFIED CONSTRUCTION OF SYMMETRIC k -LOCAL CIRCUITS FOR QCA

In this section, we show that locality-preserving unitary operators, also known as QCA [22], can be implemented as FDQC_k s. We give a generic construction of these FDQC_k s that works in any spatial dimension d . We deal only with translationally invariant QCA, but this condition can likely be relaxed to a certain extent. We also assume the QCA acts on a lattice with mirror symmetry in all d directions.

An FDQC is a trivial example of a QCA. However, there are also QCA that cannot be expressed as an FDQC , such as the 1D shift QCA Q_S , which acts on any operator O_i supported on site i by translating it by one site, $Q_S O_i Q_S^{-1} = O_{i+1}$. When only local gates are used, implementation of this operation requires a QC whose depth grows linearly with system size. In one and two dimensions, it has been shown that all QCA are composed of shifts and FDQC s [23,24]. In three dimensions, however, there are believed to be QCA that are neither shifts nor circuits [25–27]. Our result constructs FDQC_k s for all QCA, which, to the best of our knowledge, provides the first circuit representation of nontrivial 3D QCA. The existence of these FDQC_k s implies that all QCA become trivial in the k -local scenario, such that the topological classification of QCA collapses to a single trivial phase when k -local gates are allowed. Additionally, if the QCA commutes with some global symmetry, it may not be possible to write it as a *symmetric* FDQC , even if it is an FDQC . Nonetheless, the FDQC_k we construct consists of symmetric gates (in the case of global symmetries), so this result gives an alternative demonstration of the triviality of SPT order by applying our construction to the QCA that generate the SPT states, such as those in Eqs. (2) and (5).

The main ideas which lead to this result are the following. Given a QCA Q acting in d spatial dimensions, we start with the known fact that $Q \otimes Q^{-1}$ acting on two copies of a system can be realized by an FDQC [22,60]. By truncating this FDQC to a finite region of space, we obtain a k -local circuit acting on a single conjoined system. On one half of this system, the circuit acts like Q , while on the other half, it acts like Q^{-1} . We then show that Q^{-1} is equivalent to the spatial inversion of Q in one direction, which we denote as \bar{Q} , up to a circuit of $(d-1)$ -dimensional

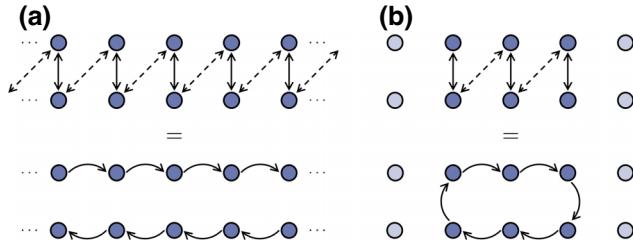


FIG. 4. (a) A pair of counterpropagating 1D QCA implementing the SHIFT operation, where information flows in the directions of the arrows, can be realized by a depth-2 k -local circuit of SWAP gates, indicated by double-headed arrows, where all solid arrows first act in parallel and then all dotted arrows act in parallel. (b) Truncation of the circuit in (a) stitches the top and bottom lines of qubits into a single ring acted on by the shift QCA.

QCA that can be applied in two parallel layers. The action of Q on one half and \bar{Q} on the other half is nothing more than Q applied to a periodic system. An inductive argument then concludes that Q can be implemented as an FDQC $_k$. This idea is demonstrated in Fig. 4 for the simple example of the shift QCA. In this case, the second part of the argument is not needed as \bar{Q} is already equal to Q^{-1} . We work out three explicit examples of the general construction, including the shift QCA, in Appendix B.

A. Construction from the 1D Margolus representation

Consider a QCA Q that acts on a Hilbert space $\mathcal{H} = (\mathbb{C}^d)^{\otimes N}$. Now construct a doubled Hilbert space $\mathcal{H}_A \otimes \mathcal{H}_B$ made of two copies of \mathcal{H} . For every degree of freedom i in \mathcal{H} , we have two degrees of freedom $[i]_A$ and $[i]_B$ in $\mathcal{H}_A \otimes \mathcal{H}_B$. Let Q_A (Q_B) denote Q acting on \mathcal{H}_A (\mathcal{H}_B) and write $V = Q_B^{-1}Q_A$. Now write $S_{AB} = \prod_i S_i$, where S_i is the SWAP operation that exchanges sites $[i]_A$ and $[i]_B$. For now, we imagine that A and B are geometrically close such that S_i is a local operator. Then we have [22,60]

$$\begin{aligned} V &= Q_B^{-1}Q_A \\ &= S_{AB}Q_A^{-1}S_{AB}Q_A \\ &= \left(\prod_i S_i \right) \left(\prod_i V_i \right), \end{aligned} \quad (10)$$

where

$$V_i = Q_A^{-1}S_iQ_A. \quad (11)$$

Since S_i is a local operator and Q is locality preserving, V_i is a local operator. Since the V_i all commute with each other for all i , the above formula can be parallelized into a finite-depth circuit realizing V .

Now we imagine truncating the above circuit as follows:

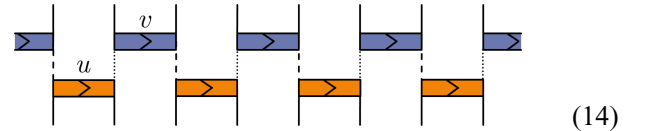
$$V_R = \left(\prod_{i \in R} S_i \right) \left(\prod_{i \in R} V_i \right), \quad (12)$$

where R is some finite connected subset of sites. Far outside the region R , V_R will act as the identity. Deep inside the region R , V_R will act as $Q_A Q_B^{-1}$. To understand what happens near the boundaries of R , we use the so-called Margolus representation of a QCA. We first describe this for 1D systems and then show how to extend it to higher-dimensional systems in the next section.

Take the physical space to be a 1D chain with sites indexed by a single integer i . By blocking a finite number of sites, i.e., enlarging the unit cell, one can always make Q have unit range, meaning that if O_i is an operator supported on a site i , then QO_iQ^{-1} is supported at most on sites $i-1, i, i+1$. Then, according to the results in Ref. [61], the QCA can be written in the following Margolus representation:

$$Q = \left(\prod_i v_{2i-1,2i} \right) \left(\prod_i u_{2i,2i+1} \right), \quad (13)$$

where u is a unitary operator mapping from the d^2 -dimensional Hilbert space $\mathbb{C}^d \otimes \mathbb{C}^d$ to the ℓr -dimensional Hilbert space $\mathbb{C}^\ell \otimes \mathbb{C}^r$, where d is the dimension of a unit cell and $\ell r = d^2$. Similarly, v is a unitary operator mapping from $\mathbb{C}^r \otimes \mathbb{C}^\ell$ to $\mathbb{C}^d \otimes \mathbb{C}^d$. Graphically, we can represent the right-hand side of this equation as follows (where the solid, dashed, and dotted lines have dimensions d , ℓ , and r , respectively):



The arrows indicate the orientation of the unitaries u and v and are expressed formally by the spatial ordering of the Hilbert space labels on the left and the right. This will become important when we invert this orientation, as we define shortly. The standard form encompasses all 1D QCA, even the shift QCA, whose standard form is described in Appendix B 1.

We emphasize that the ℓ -dimensional and r -dimensional Hilbert spaces are not physical, and are rather a technical tool used to write the Margolus representation. Accordingly, the operators u and v are not proper unitary gates, since their input and output Hilbert spaces are not equivalent. Rather, they are used as building blocks to define proper unitary gates such as Q itself.

We now insert the standard form of Q into the definition of V_R , where we take R to be a segment of the 1D line

$R = [c, d]$. Without loss of generality, suppose that c is odd and d is even such that the length of R is even. We then have

$$\begin{aligned}
V_R &= \left(\prod_{i=c}^d S_i \right) \left(\prod_{i=c}^d V_i \right) \\
&= \left(\prod_{i=c}^d S_i \right) Q_A^{-1} \left(\prod_{i=c}^d S_i \right) Q_A \\
&= \left(u_{[c-1]_A, [c]_B}^{-1} u_{[d]_B, [d+1]_A}^{-1} \right) \\
&\quad \times \left(\prod_{i=\frac{c+1}{2}}^{d/2-1} u_{[2i]_B, [2i+1]_B}^{-1} \right) \left(\prod_{i=\frac{c+1}{2}}^{d/2} v_{[2i-1]_A, [2i]_A} \right) \\
&\quad \times \left(\prod_{i=\frac{c+1}{2}}^{d/2} v_{[2i-1]_B, [2i]_B}^{-1} \right) \left(\prod_{i=\frac{c-1}{2}}^{d/2} u_{[2i]_A, [2i+1]_A} \right) \quad (15)
\end{aligned}$$

The second and third equalities above are depicted on the left and middle of Fig. 5, respectively. As is clear from Fig. 5, the u , u^{-1} , v , v^{-1} operators can be parallelized into two layers of disjoint operators. Namely, the u and v^{-1} operators can act in parallel in the first layer, and the v and u^{-1} operators act in the second layer. Furthermore, we see that the degrees of freedom within the range $[c-1, d+1]$ have been stitched into a single periodic 1D system, a ring of length $L = 2(d-c+1) + 2$ with spins in the subsystem A (B) forming the “front” (“back”) of the ring that we denote as \mathcal{R} . Whenever we use the notation \mathcal{R} , we imagine it as representing a finite periodic array of sites that can be ordered counterclockwise as $[c]_A, \dots, [d+1]_A, [d]_B, [d-1]_B, \dots, [c]_B, [c-1]_A$.

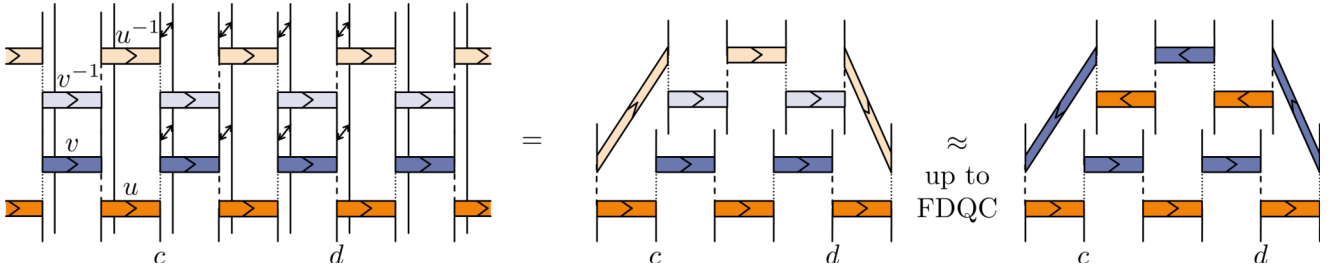


FIG. 5. The truncated circuit V_R , where the 1D QCA Q is expressed in standard form. The downwards-shifted (upwards-shifted) vertical lines correspond to degrees of freedom in the subsystem A (B). The lighter-colored rectangles represent the inverses u^{-1} and v^{-1} as indicated in the first diagram. An arrow between two lines indicates the SWAP operation S_i between degrees of freedom in the two subsystems. In the second diagram, most gates have canceled pairwise, leaving only those shown. The degrees of freedom acted on by the remaining gates form the ring \mathcal{R} . For visual clarity, the vertical lines have been shortened. The third diagram is equivalent to the second diagram up to the symmetric FDQCs W_1 and W_2 ; see Eq. (18). Note that the strict equivalence up to symmetric FDQCs is in one spatial dimension, $d = 1$. In higher dimensions ($d > 1$), we use the compactified picture such that the equivalence is up to a circuit that is of finite depth along the noncompactified direction and, in general, a $(d-1)$ -dimensional QCA along the $d-1$ compactified directions; see the main text.

The operator V_R is not exactly Q acting on the finite periodic system defined by \mathcal{R} , which is depicted in the third diagram in Fig. 5. Instead, V_R realizes Q on the front of \mathcal{R} and \bar{Q}^{-1} on the back of \mathcal{R} , with the two operators being blended near the edges. To fix this, we show that V_R is equivalent to Q up to composition with an FDQC. Given any 1D QCA Q , we show that its inverse Q^{-1} is related to its orientation-reversed self \bar{Q} by an FDQC. This is intuitively clear for 1D QCA such as the shift QCA: reversing the direction of the shift is the same as inverting it. Generally, \bar{Q} will not equal Q^{-1} , but they will differ only by an FDQC in one dimension [62].

To explicitly construct the circuit that maps \bar{Q} to Q^{-1} , we introduce the unitary $w = \bar{v}u$, where \bar{v} is the spatial reversal (opposite orientation) of v obtained by exchanging the left and right input and output Hilbert spaces. That is, $v_{i,j} = \bar{v}_{j,i}$. Graphically,

$$w = \begin{array}{c} \text{---} \leftarrow \text{---} \\ \text{---} \rightarrow \text{---} \end{array} \quad (16)$$

Note that w , unlike u and v , is a proper unitary gate that maps $\mathbb{C}^d \otimes \mathbb{C}^d$ to itself. Observe that we have $wu^{-1} = \bar{v}$ and $v^{-1}\bar{w} = \bar{u}$, where \bar{w} is again the spatial reversal of w . Then we have

$$\left(\prod_i w_{2i, 2i+1} \right) Q^{-1} \left(\prod_i \bar{w}_{2i-1, 2i} \right) = \bar{Q}. \quad (17)$$

Since the $w(\bar{w})$ gates on either side of Q^{-1} are non-overlapping, they can be applied in parallel. Therefore, Q^{-1} and \bar{Q} are related by composition with FDQCs. Using

this, we define the circuits acting on the “back” of \mathcal{R} ,

$$W_1 = (w_{[c-1]_A, [c]_B} w_{[d]_B, [d+1]_A}) \left(\prod_{i=\frac{c+1}{2}}^{d/2-1} w_{[2i]_B, [2i+1]_B} \right),$$

$$W_2 = \left(\prod_{i=\frac{c+1}{2}}^{d/2} \bar{w}_{[2i-1]_B, [2i]_B} \right),$$
(18)

such that

$$W_1 V_R W_2 = (\bar{v}_{[c-1]_A, [c]_B} \bar{v}_{[d]_B, [d+1]_A})$$

$$\times \left(\prod_{i=\frac{c+1}{2}}^{d/2-1} \bar{v}_{[2i]_B, [2i+1]_B} \right) \left(\prod_{i=\frac{c+1}{2}}^{d/2} v_{[2i-1]_A, [2i]_A} \right)$$

$$\times \left(\prod_{i=\frac{c+1}{2}}^{d/2} \bar{u}_{[2i-1]_B, [2i]_B} \right) \left(\prod_{i=\frac{c-1}{2}}^{d/2} u_{[2i]_A, [2i+1]_A} \right).$$
(19)

The operator $W_1 V_R W_2$ is shown in the third diagram in Fig. 5, from which it is clear that $W_1 V_R W_2$ is nothing but Q applied to \mathcal{R} . According to the 1D ring topology of \mathcal{R} , V_R is not geometrically local since it contains gates coupling qubits on opposite sides of \mathcal{R} . However, it is still k local. Therefore, $W_1 V_R W_2$ is an FDQC_k that realizes Q on a finite ring, where Q is an arbitrary 1D QCA. The elementary gates that make up the FDQC_k are S_i , V_i , and w . In Appendix B, we derive these gates and demonstrate the general construction for several explicit examples.

B. Application to compactified higher-dimensional systems

Having shown that all 1D QCA can be realized as an FDQC_k , we now move on to higher-dimensional QCA acting on d -dimensional lattices. For simplicity, we assume we have a simple hypercubic lattice structure, although the construction should generalize to any translationally invariant QCA on a lattice with mirror symmetries. We also assume without loss of generality that the QCA has a unit range in all d directions. It is known that a local Margolus form is not possible for 2D and higher-dimensional QCA [63]. However, we can still obtain the desired results by applying the 1D Margolus representation, which was also used to understand the index theory of higher-dimensional QCA [24]. To do this, we simply compactify the d -dimensional QCA Q along all spatial dimensions except for one to obtain a quasi-1D chain of supersites i each containing a number of sites that is extensive in the $d-1$ compactified dimensions. Since Q has

a unit range, it will spread operators contained in supersite i only to supersites $i-1, i, i+1$ such that Q can be viewed as a 1D QCA of unit range acting on the compactified system. Therefore, it may be written in the Margolus representation of Eq. (14), where each solid vertical line now represents one supersite.

Application of the construction described above then automatically gives an FDQC_k on the supersites realizing Q . However, we must be careful to confirm that the depth of the k -local circuit and the value of k are both independent of system size in the compactified dimensions. This is clearly true of V_R , whose definition in Eq. (12) is unaffected by the compactification and hence it is still k local and of finite depth. Note that while the definition of V_R depends on which dimensions we choose to compactify, V_R is unaffected by whether we actually compactify those dimensions. What remains then is to check that the unitary w used to define W_1 and W_2 can be realized as an FDQC_k . Note that W_1 and W_2 consist of a parallel application of w . Then, if w can be realized as an FDQC_k , so can W_1 and W_2 . We show that this is the case by showing that w is in fact a $(d-1)$ -dimensional QCA and then using an inductive argument.

We now show that w is locality preserving as well as translationally invariant in the compactified dimensions, i.e., it is a $(d-1)$ -dimensional QCA. Let O be a local operator. Recall that $w = \bar{v}u$. Let $uOu^{-1} = \sum_k A^k \otimes B^k$, where A^k and B^k are operators supported only on the ℓ -dimensional and r -dimensional Hilbert spaces that come out of u , respectively. Using the Schmidt decomposition, we can always choose A^k (B^k) to come from a linearly independent set of operators acting on \mathbb{C}^ℓ (\mathbb{C}^r). Let $C^k = \bar{v}A^k\bar{v}^{-1}$ and $D^k = \bar{v}B^k\bar{v}^{-1}$. Note that since v is a unitary map and since A^k and B^k were linearly independent, C^k and D^k are linearly independent as well. Then from linearity, we have

$$wOw^{-1} = \sum_k C^k D^k. \quad (20)$$

As we show below, the locality-preserving property of the original QCA Q ensures that each C^k and D^k in this sum is localized around O (meaning that they all are contained in a ball of finite radius centered at O), and thus w is locality preserving.

Consider the action of Q on O . In the following calculation, we will be more explicit with site indices; we write $O_{2i, 2i+1}$ to represent the two (super)site operators O acting on (super)sites $2i$ and $2i+1$. Then

$$QO_{2i, 2i+1}Q^{-1}$$

$$= \left(\prod_j v_{2j-1, 2j} \right) \sum_k A_{2i}^k \otimes B_{2i+1}^k \left(\prod_j v_{2j-1, 2j}^{-1} \right)$$

$$\begin{aligned}
&= \sum_k (v_{2i-1,2i} A_{2i}^k v_{2i-1,2i}^{-1}) \otimes (v_{2i+1,2i+2} B_{2i+1}^k v_{2i+1,2i+2}^{-1}) \\
&= \sum_k \bar{C}_{2i-1,2i}^k \otimes \bar{D}_{2i+1,2i+2}^k, \tag{21}
\end{aligned}$$

In the first equation, we used the Margolus representation of Q and conjugated O by the u operators. The bars appearing on C^k and D^k again indicate spatial reversal since A^k and B^k have been conjugated by v rather than \bar{v} . As shown in Appendix C, since $QO_{2i,2i+1}Q^{-1}$ is contained around O , linear independence ensures that each \bar{C}^k and \bar{D}^k should be contained around O . This, in turn, shows that wOw^{-1} in Eq. (20) is also contained around O , and hence w is also locality preserving in the $d-1$ compactified dimensions. A similar argument shows that w is translationally invariant in the compactified directions if Q is (see Appendix C for details). In other words, w is a $(d-1)$ -dimensional QCA.

We finish the proof using an inductive argument. We have already explicitly shown how to realize any 1D QCA as an FDQC_k . Now suppose we can realize any d -dimensional QCA as an FDQC_k . Then, given a $(d+1)$ -dimensional QCA Q , we have shown how to prepare it using the FDQC_k V_R and the unitary w . Since w is a d -dimensional QCA, we can by assumption realize it, and hence Q itself, as an FDQC_k . We note that w is not an FDQC in general, so this inductive step is necessary. For example, if we consider the 2D QCA that shifts operators diagonally, then w will be a 1D shift QCA, as demonstrated in Appendix B 3.

C. Symmetric QCA and SPT phases

We now turn to the symmetry properties of the FDQC_k s constructed in the previous section. Suppose Q is a symmetric QCA, meaning that it commutes with a *global* symmetry $U(g) = u(g)^{\otimes N}$ for $g \in G$ (we discuss higher-form symmetries at the end). Note that, in contrast to a symmetric QC, where each gate in the circuit is individually symmetric, here we don't necessarily have a way to break Q into smaller pieces, so we require only that Q as a whole is symmetric, $[Q, U(g)] = 0$. Let $U_A(g)$ ($U_B(g)$) denote $U(g)$ acting on the subsystem A (B) as defined in the previous section. $U_A(g)U_B(g)$ clearly commutes with the SWAP operators S_i , since it is a tensor product of the same operator $u(g)$ on every site. Given that Q_A is assumed to be symmetric, $V_i = Q_A S_i Q_A^{-1}$ commutes with $U_A(g)U_B(g)$ as well, and thus all gates in the circuit V_R defined in Eq. (12) commute with $U_A(g)U_B(g)$ for all $g \in G$. When we view the sites acted on by V_R as the ring \mathcal{R} , $U_A(g)U_B(g)$ is just $U(g)$ acting on all sites in the ring, so it is just the global symmetry of the ring, which we denote as $U_{\mathcal{R}}(g)$. For $c \leq i \leq d$, V_i and S_i have trivial support outside \mathcal{R} , and hence the fact that they commute with $U_A(g)U_B(g)$ readily shows that they also commute with $U_{\mathcal{R}}(g)$. Next, it follows

from the results in Ref. [64] that w commutes with $U(g)$ for all $g \in G$; see Appendix C for details. Therefore, $W_1 V_R W_2$ is a symmetric FDQC_k whose gates commute with $U_{\mathcal{R}}(g)$ for all $g \in G$.

This result has implications for SPT phases. Observe that the FDQC_k s used to disentangle the SPT fixed-point states in Sec. III generate the same unitary operators as the nonsymmetric FDQC s used to define the states in the first place, which we call ‘‘SPT entanglers.’’ That is, our constructions did not just trivialize the fixed-point states, they achieved the stronger task of expressing the SPT entanglers themselves as symmetric FDQC_k s. This perspective allows us to apply our results on representing QCA as symmetric FDQC_k s to SPT phases. For example, fixed-point states for a large class of bosonic SPT phases (the ‘‘in-cohomology’’ phases) with global symmetry are given by the cocycle states defined in Ref. [7]. These states are, in turn, defined by FDQC s that commute with the global symmetry, but they are not symmetric circuits since the individual gates are not symmetric. Our construction allows these circuits to be written as FDQC_k s with symmetric gates. This shows that all in-cohomology SPT phases are trivial in the k -local scenario. We demonstrate this idea for the example of the 1D cluster state in Appendix B 2.

Our construction can be applied to some beyond-cohomology SPT phases as well, although these are less well understood at the Hamiltonian level. One example of a beyond-cohomology SPT phase in four dimensions with \mathbb{Z}_2 symmetry was given in Ref. [29], which also constructed a \mathbb{Z}_2 -symmetric SPT entangler. This entangler is an FDQC , so our construction can be applied to get a symmetric FDQC_k . An interesting direction for further work requires extending our results to consider antiunitary symmetries, i.e., time reversal, which would allow us to address the k -local triviality of the 3D beyond-cohomology phase in Ref. [65].

Finally, we note that our approach immediately fails for higher-form symmetries. This is because the gates in V_R commute only with $U_A(g)U_B(g)$ and do not commute with $U_A(g)$ or $U_B(g)$ individually. That is, the only symmetry operators that commute with V_R are those that act in the same way on the front half and the back half of \mathcal{R} . However, the full higher-form symmetry group includes operators that act differently on the two halves, as discussed in Sec. III D. So V_R does not commute with the full higher-form symmetry group.

V. STABILITY OF SPT PHASES UNDER GENERIC k -LOCAL INTERACTIONS

In the previous section, we showed the existence of symmetric FDQC_k s that trivialize SPT phases. However, as these circuits are fine-tuned, this does not necessarily imply that SPT phases are unstable to *generic* symmetric

k -local interactions. Here we argue that this is the case, meaning that generic symmetric k -local interactions will destroy SPT order. We first consider specific instances of interactions, and then we argue why the same results should hold generically.

We focus on the case of 1D SPT phases, but we expect that similar arguments will carry over to higher dimensions as well. We take $|\psi_C\rangle$ [Eq. (2)] as the fixed-point state in a nontrivial SPT phase and construct perturbed states $|\psi\rangle$ by applying a short time-independent Hamiltonian time evolution $|\psi\rangle = e^{-iH}|\psi_C\rangle$ for some H . We consider several choices of H subjected to certain locality and symmetry constraints. By taking t to be arbitrarily small, this gives a perturbed state that is arbitrarily close to the unperturbed state (in terms of fidelity per site). Therefore, we consider this a model of the effect of weak k -local noise on an SPT phase, which may or may not destroy the SPT order. This is in contrast to our exact disentangling FDQC $_k$ s obtained in Sec. III, which require strong k -local interactions.

To diagnose the presence or absence of SPT order in the resulting state, we use the string order parameter [66], which can be defined as

$$S(a, b) = Z_a Y_{a+1} \left(\prod_{i=a+2}^{b-1} X_i \right) Y_b Z_{b+1}. \quad (22)$$

In the nontrivial SPT phase containing $|\psi_C\rangle$, the string order generically saturates to a nonzero value as its length is increased, whereas it goes to zero exponentially quickly in the trivial phase. In particular, we have $\langle \psi_C | S(a, b) | \psi_C \rangle = 1$. To reduce the number of length scales, we evaluate the string order parameter over half of the system, i.e., $S := S(0, N/2)$, and study its behavior as a function of the system size N .

We first consider local, asymmetric noise, generated by the Hamiltonian $H^{(1)} = -\sum_i Z_i$. Since Z_i anticommutes with some symmetry generators of $|\psi_C\rangle$, this is not a symmetric Hamiltonian. Therefore, we expect that the time-evolved state will be in a trivial SPT phase and the string order will decay exponentially to zero with increasing N . The state after an evolution time t is

$$|\psi^{(1)}\rangle = \prod_{i=1}^N e^{itZ_i} |\psi_C\rangle. \quad (23)$$

We define the subset of sites $\mathcal{I} = \{1, 2, \dots, N/2\}$, which has the property that Z_i anticommutes with S if $i \in \mathcal{I}$ and commutes with S otherwise. Then we can straightforwardly evaluate the string order in this perturbed state:

$$\langle \psi^{(1)} | S | \psi^{(1)} \rangle = \langle \psi_C | \left(\prod_{i=1}^N e^{-itZ_i} \right) S \left(\prod_{i=1}^N e^{itZ_i} \right) | \psi_C \rangle$$

$$\begin{aligned} &= \langle \psi_C | \left(\prod_{i \in \mathcal{I}} e^{-2itZ_i} \right) S | \psi_C \rangle \\ &= \langle \psi_C | \prod_{i \in \mathcal{I}} (\cos 2t - i \sin 2t Z_i) | \psi_C \rangle \\ &= \gamma^{N/2}, \end{aligned} \quad (24)$$

where $\gamma = \cos 2t$ and we used the facts that $S|\psi_C\rangle = |\psi_C\rangle$ and $\langle \psi_C | \prod_{i \in \mathcal{S}} Z_i | \psi_C \rangle = 0$ for any nonempty index set \mathcal{S} . Since $\gamma < 1$ for any nonzero $t \ll 1$, we see that the string order decays to zero exponentially quickly, indicating that the state $|\psi^{(1)}\rangle$ has trivial SPT order.

We repeat the same calculation for a symmetric, local Hamiltonian. We choose the perturbation $H^{(2)} = -\sum_i Z_{i-1} Z_{i+1}$, which commutes with the $\mathbb{Z}_2 \times \mathbb{Z}_2$ symmetry. The time-evolved state is

$$|\psi^{(2)}\rangle = \prod_{i=1}^N e^{itZ_{i-1}Z_{i+1}} |\psi_C\rangle. \quad (25)$$

The calculation of string order is largely the same. The key difference is that the set of sites i for which $Z_{i-1}Z_{i+1}$ anticommutes with S is finite, containing only sites $i = 0, 1, N/2, N/2 + 1$. Therefore, we find that

$$\langle \psi^{(2)} | S | \psi^{(2)} \rangle = \gamma^4, \quad (26)$$

so the string order is a nonzero constant independent of N , indicating that $|\psi^{(2)}\rangle$ has nontrivial SPT order, as expected.

Finally, we consider the case of k -local symmetric perturbations. On the basis of the disentangling circuits we constructed in the previous sections, we expect that this will trivialize the SPT order. We define a set \mathcal{A} consisting of random pairings of sites (i, j) such that every site is contained in exactly one pair, and i and j are either both even or both odd. Then we consider the 2-local symmetric perturbation $H^{(3)} = -\sum_{(i,j) \in \mathcal{A}} Z_i Z_j$. We could also consider the case where every qubit interacts pairwise with every other qubit, but the calculation is greatly simplified by assuming each qubit interacts only with one other qubit. Note also that this Hamiltonian has constant energy density despite being long-range interacting. As before, we consider the state

$$|\psi^{(3)}\rangle = \prod_{(i,j) \in \mathcal{A}} e^{itZ_i Z_j} |\psi_C\rangle. \quad (27)$$

We now split \mathcal{A} into two subsets \mathcal{A}_e and \mathcal{A}_o such that $(i, j) \in \mathcal{A}_e$ if i and j are both in \mathcal{I} or neither is, while $(i, j) \in \mathcal{A}_o$ if one of i and j is in \mathcal{I} and the other is not. Then $Z_i Z_j$ anticommutes with S if and only if $(i, j) \in \mathcal{A}_o$.

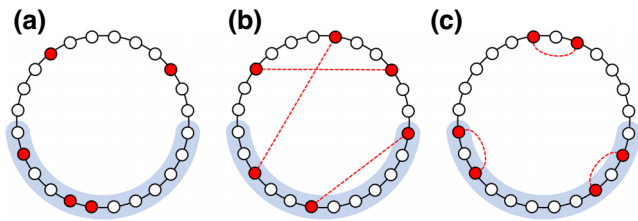


FIG. 6. Typical components of the perturbed states for (a) random, (b) symmetric k -local, and (c) symmetric local perturbations. Each red circle denotes the application of one Z operator, and the dashed lines connecting two circles represent symmetric pairs of Z operators. The shaded regions indicate the region over which the string order is evaluated. In a typical configuration, (c) will likely have an even number of Z operators in the shaded region, whereas (a) and (b) have no parity bias.

Following the above calculations, we find

$$\langle \psi^{(3)} | S | \psi^{(3)} \rangle = \gamma^{|\mathcal{A}_o|}, \quad (28)$$

where $|\mathcal{A}_o|$ is the number of pairs in \mathcal{A}_o . Given a random pairing of sites described by the set \mathcal{A} , if we take any site $i \in \mathcal{I}$, its partner will be in \mathcal{I} with probability approximately $1/2$ since \mathcal{I} contains half of the lattice sites. Therefore, we expect for typical pairings that $|\mathcal{A}_o| \approx N/4$ (as $|\mathcal{A}| = N/2$), so the string order decays exponentially with increasing N , indicating trivial SPT order.

The above analysis makes it clear why symmetric k -local perturbations destroy SPT order. Consider the two states $|\psi^{(1)}\rangle$ and $|\psi^{(3)}\rangle$. Each is a superposition over states of the form $\propto \prod_{i \in \mathcal{S}} Z_i |\psi_C\rangle$ for some index sets \mathcal{S} . The only significant difference between the two states is that in the case of $|\psi^{(3)}\rangle$, the global symmetry constraint requires $\prod_{i \in \mathcal{S}} Z_i$ to contain an even number of Z 's on both sublattices. However, the string order parameter, which is evaluated only over half of the lattice sites, does not see this global constraint; there is a high probability for an odd number of Z 's to be applied to the region where the string order parameter acts; see Fig. 6. This anticommutation of the perturbations with the string order parameter leads to destructive interference, which causes it to decay. In contrast, in $|\psi^{(2)}\rangle$, the Z 's always appear in pairs separated by a short distance, such that only those pairs that straddle the boundary of \mathcal{I} will anticommute with S , which gives only a finite correction to the string order; see Fig. 6. In other words, the k -local symmetric perturbations allow one to freely violate the symmetry in any local region, and this is what leads to the breakdown of the SPT order. Indeed, the value of the string order parameter within any region in which the symmetry is violated necessarily goes to zero [67]. From this reasoning, it is clear that any generic k -local perturbation will similarly destroy SPT order.

On the other hand, if the k -local perturbation is *locally symmetric*, meaning that the perturbation has a form such as $O_i O_j$, where O_i and O_j are symmetric local operators, then this does not violate the symmetry locally, and we expect the SPT order will be robust to such perturbations. This symmetry restriction is the same as the symmetry restriction for higher-form SPTs as discussed in Sec. III D.

A. Instability of SPT states in monitored random circuits

We have argued that SPT order is unstable to generic k -local symmetric perturbations but it is stable to k -local perturbations that are locally symmetric. In this section, we give further numerical evidence of these claims. We consider monitored quantum circuits, which involve both unitary gates and projective measurements that are randomly applied to the state with some probability (for a review, see Ref. [68]). In general, it has been observed that these elements compete with each other, driving the late-time state of the evolution to different regimes of behavior depending on their relative frequency. In particular, certain symmetric monitored random circuits have been studied that can sustain SPT order within a certain range of the circuit parameters [69,70]. We study the implication of our results for the stability of SPT order in this context and use this to give further evidence on which k -local circuits can and cannot trivialize SPT phases.

Consider arranging N qubits, initialized in the $|+\rangle^{\otimes N}$ state, on a 1D ring and applying the following quantum process: at each step, with probability p a random two-qubit unitary U is applied to the system or, with probability $1-p$ a qubit i is chosen uniformly at random and $g_i \equiv Z_{i-1} X_i Z_{i+1}$ is measured. The latter tends to drive the state towards the 1D cluster state that satisfies $g_i |\psi_C\rangle = |\psi_C\rangle$, while the former tends to drive it away. A time step is defined to consist of N consecutive steps. In the following, we consider four different ensembles of two-qubit unitaries: (1) all two-qubit geometrically local Clifford unitaries, (2) two-qubit geometrically local Clifford unitaries that respect the $\mathbb{Z}_2 \times \mathbb{Z}_2$ symmetry generated by X_{odd} and X_{even} , (3) 2-local Clifford unitaries that respect the same $\mathbb{Z}_2 \times \mathbb{Z}_2$ symmetry, and (4) 2-local Clifford unitaries that respect the \mathbb{Z}_2^N symmetry generated by X_i for $i = 1, \dots, N$, i.e., that are diagonal in the local X basis and are therefore locally symmetric. In the case of geometrically local unitaries, a site i is chosen at random, and a two-qubit unitary, chosen randomly from the appropriate ensemble, is applied to qubits i and $i+1$. As for 2-local unitaries, two different sites i and j are chosen randomly and then a random unitary from the appropriate ensemble is applied to them. We are interested in the late-time states of this family of random circuits, which we take to be the quantum state of the circuit after $T = N$ time steps.

At $p = 0$, the circuit consists of only g_i stabilizer measurements. Therefore, the late-time state of any realization of the random circuit would be an SPT state. The SPT nature of this state can be probed by the non-local analogue of the Edwards–Anderson glass-order parameter [69,71,72]:

$$s = \frac{2}{N(N-1)} \sum_{a < b} S(a,b)^2, \quad (29)$$

with $S(a,b)$ being the SPT string order parameter defined in Eq. (22). $s = 1$ for $|\psi_C\rangle$. As described earlier, SPT states are characterized by $s > 0$, while for trivial states or random states, $s = 0$ in the thermodynamic limit. We are interested in \bar{s} , which is s averaged over random circuit realizations. We note that s is not an *experimentally* accessible quantity, but it is certainly accessible in simulations, which is sufficient for our present purposes.

Figure 7 shows \bar{s} as a function of p for each of the unitary ensembles described above. Figure 7(a) corresponds to the random circuit where the unitary gates are chosen from the ensemble of local two-qubit Clifford gates without our imposing any symmetry restriction. As expected, the SPT structure in the late-time state vanishes for any $p > 0$ as the symmetry is violated. On the other hand, if we restrict the local unitary gates to respect the $\mathbb{Z}_2 \times \mathbb{Z}_2$ symmetry, the SPT structure survives up to finite $p_c > 0$, below which \bar{s} saturates to a finite value, as shown in Fig. 7(b). Interestingly, when the unitary gates are chosen from the set of 2-local Clifford unitaries that respect the $\mathbb{Z}_2 \times \mathbb{Z}_2$ symmetry, the SPT structure vanishes again for any $p > 0$, as illustrated in Fig. 7(c). This is consistent with our findings that SPT states can be trivialized by k -local symmetric unitary gates. Lastly, Fig. 7(d) corresponds to the circuit where the unitary gates are chosen from the highly constrained ensemble of 2-local Clifford unitaries that map X_i to itself for all i , i.e., they are locally symmetric. Despite the fact that this set includes long-range entangling gates, we see that the SPT structure survives up to finite $p > 0$, which is consistent with our intuition that k -local gates that are locally symmetric are not much more powerful in terms of disentangling the SPT structure than geometrically local symmetric gates. In Appendix E we provide further analysis of the numerical data shown in Fig. 7

VI. DISCUSSION

We have constructed explicit finite-depth circuits consisting of (symmetric) k -local gates to create fixed-point SPT states and to realize all QCA. The circuits imply that the classification of SPT phases (with global or subsystem symmetries) and the classification of QCA collapse to a single trivial phase in the presence of k -local interactions. This addresses *worst-case stability*—whether there exists an FDQC of k -local gates that can trivialize a

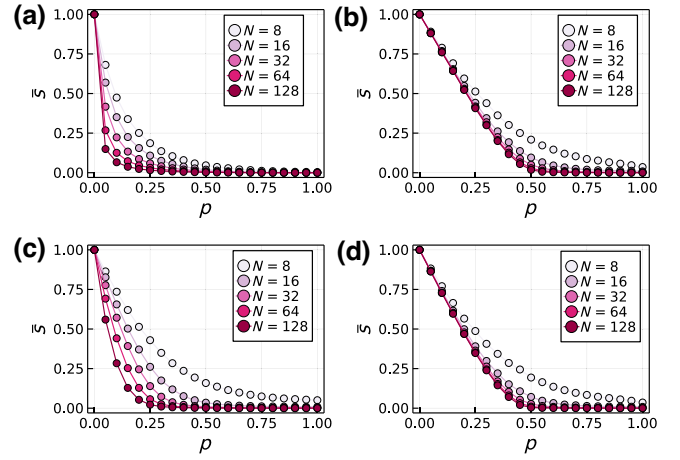


FIG. 7. Averaged string order parameter \bar{s} versus p for monitored random circuits where the unitary gates are chosen randomly from (a) local two-qubit Clifford unitaries, (b) local two-qubit $\mathbb{Z}_2 \times \mathbb{Z}_2$ symmetric Clifford unitaries, (c) 2-local $\mathbb{Z}_2 \times \mathbb{Z}_2$ symmetric Clifford unitaries, and (d) 2-local \mathbb{Z}_2^N symmetric Clifford unitaries.

given state—and suffices to show that these phases (strictly speaking) do not exist in the presence of k -local interactions. We also addressed the case of *typical case stability* by giving analytical and numerical evidence that SPT order is also fragile in the presence of generic k -local symmetric perturbations. We note that a key ingredient in our explicit circuits was to “fold” the system in such a way that it resembled a stack of the system with its inverted self. This naturally assumes some sort of mirror symmetry is present in the lattice. Therefore, it is natural to ask whether our results can be applied to systems on more general lattices and to what extent translational invariance can be relaxed.

We remark that SPT phases can be used as resources for measurement-based quantum computation (MBQC); see Ref. [73] for a review. That is, given a ground state in a suitable SPT phase, one can perform measurements on that ground state so as to simulate a quantum computation. While the computational capability of a state as a resource for MBQC is stable to local symmetric perturbations, our results seem to imply that it may be unstable to k -local symmetric perturbations in the case of global or subsystem symmetries. Indeed, Raussendorf *et al.* [52] explicitly identified a symmetric k -local interaction whose presence would invalidate the strategy that was used to prove MBQC universality. In contrast, fault-tolerant MBQC can be achieved with use of SPT phases with higher-form symmetries [74], which appear to be stable even under symmetric k -local interactions.

While we have focused on bosonic systems, we believe that many of our arguments should apply to fermionic systems as well. Indeed, our physical arguments for the triviality of SPT phases based on their boundary physics and invertibility should carry over *mutatis*

mutandis. Specifically, the free fermion SPT phases (i.e., topological insulators and superconductors) are characterized by nontrivial boundary states, which are manifestly rendered trivial if one can couple distinct boundaries together via k -local interactions. Meanwhile, Wang and Senthil [75] showed that the set of fermionic SPT phases in three dimensions, protected by some combination of antiunitary symmetries and charge conservation, is exhausted by combinations of the free fermion SPTs and bosonic SPTs—and bosonic SPTs we have constructively shown to be trivialisable. This suggests that these fermion SPTs should also be trivialisable by k -local interactions. Similarly, we expect that many, if not all, fermionic QCA should become trivial in the k -local setting [31,76]. However, the establishment of rigorous results on fermionic SPTs and QCA is left to future work.

In contrast to SPT states and QCA, intrinsic topological order is known to be stable under finite-depth k -local circuits [33], meaning that a nontrivial topological phase will not become trivial. However, this does not mean that the classification of intrinsic topological phases will remain unchanged. Indeed, in the k -local scenario, it is possible that the braiding of topological excitations becomes ill-defined, so some topological phases that differ only by braiding statistics may become the same phase. Also, in symmetry-enriched topological phases, the topological order is stable but the nontrivial symmetry fractionalization pattern of the symmetry-enriched topological phase may not be stable under k -local circuits. For instance, certain symmetry fractionalization patterns can be canceled by stacking with SPT states [77]. Since we know that SPT states can be prepared with finite-depth k -local circuits, such symmetry fractionalization patterns are not stable to finite-depth k -local circuits. A thorough investigation of the stability of intrinsic topological order and symmetry fractionalization is left for future work.

Another class of phases for which the action of k -local circuits is interesting is fracton phases (for reviews, see Refs. [78–80]). The defining property of fracton phases is the restricted mobility of the excitations, which comes about because the nontrivial excitations are not locally creatable but instead arise at the “corners” of extended operators. For instance, in the X-cube model [81] the fractons arise at the corners of membrane operators. Since these excitations cannot be created (or destroyed) by any few-body operator, they cannot be moved by k -local perturbations (without creating additional excitations), and thus the restricted mobility survives. Nonetheless, not all properties of fracton phases are unchanged. For instance, the geometric nature of entanglement can be modified under k -local gates. To illustrate this, we specialize to *gapped* fracton phases, which are characterized by non-local entanglement with geometric rigidity [82–85]. We

expect that this nonlocal entanglement survives under k -local gates, much like the corresponding entanglement structure in phases with intrinsic topological order, but (we argue) the geometric structure does not survive. For instance, consider a stack of 2D toric codes. Each copy of the 2D toric code has a topological order that is stable under k -local gates that couple degrees of freedom in that copy alone. However, under a k -local circuit that couples different copies of toric codes, the foliation structure of the stack can be lost and may no longer be recoverable with use of a geometrically local FDQC; see Fig. 8(a). This argument extends to foliated fracton codes (see, e.g., Ref. [86]). Under a geometrically local FDQC, a stack of 2D topological codes, which is said to form the foliations of the fracton order, can be extracted. For extraction of one layer of a 2D model alone, the “exfoliating” circuit applies local disentangling operations on the boundary of the fracton order. However, a k -local circuit can entangle the extracted foliations back into the fracton order in a way that it can no longer be disentangled via an FDQC. In this sense, the structure of the entanglement has changed i.e., there is no exfoliation via a geometrically local FDQC. We illustrate this for the example of the X-cube model in Fig. 8(b). Similar considerations apply to the more general notion of bifurcating entanglement renormalization that has been explored for fracton orders [87,88] and SPT states [89]. A detailed exploration of fracton phases under k -local circuits is a promising topic for future work.

Our results have a bearing on the classification of chiral Floquet phases of matter. The nontrivial nature of these models is based on the fact that the effect of the Floquet dynamics at the boundary of an open system cannot be realized by an FDQC. The boundary dynamics of the models in Ref. [30] are given exactly by 1D bosonic QCA. Hence, our results show that the boundaries are no longer anomalous if k -local interactions are allowed, as 1D QCA are all FDQC $_k$ s. On the other hand, the radical Floquet phases introduced in Ref. [32] have boundary dynamics described by a shift of a Majorana fermion that has a fractional index. As such an index is beyond bosonic QCA, and the bulk model consists of bosonic degrees of freedom, it is plausible that these phases remain robust to k -local interactions unless ancillary fermionic degrees of freedom are added.

Recently, Floquet codes have also been discussed in the literature [90]. Such codes are defined by a series of instantaneous codes, each of which is an instance of intrinsic topological order. Hence, it is natural to expect that such codes are stable to k -local noise. It could also be interesting to discuss symmetry-enriched Floquet codes, bearing in mind the subtleties associated with defining symmetries for Floquet unitaries [91]

Our work can also be extended by modifying the definition of a locality-preserving unitary. One can weaken

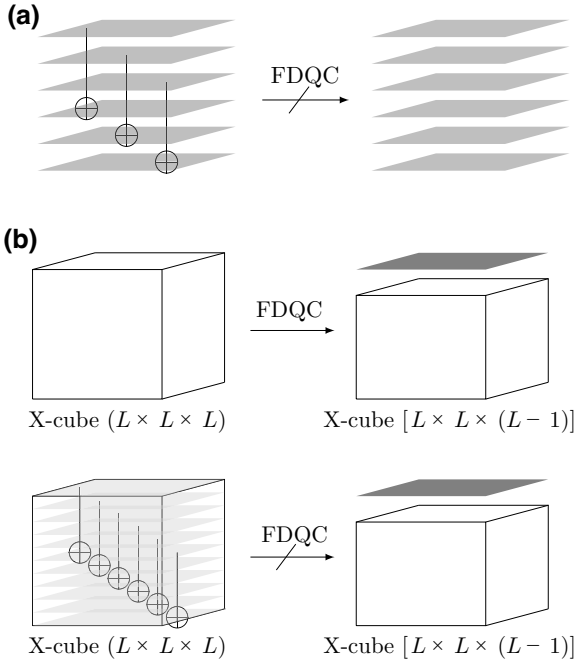


FIG. 8. (a) Action of a k -local circuit on a stack of toric codes, in general, leads to a model that is no longer a finite-depth local quantum circuit equivalent to a stack. (b) Top: The X-cube model is foliated, i.e., there exists a finite-depth local quantum circuit under which an $L \times L \times L$ X-cube model maps to an X-cube model of dimensions $L \times L \times (L - 1)$ and a layer of toric code. Bottom: Action of a k -local circuit on the X-cube model, in general, leads to a model that is no longer a finite-depth local quantum circuit equivalent to a foliated model.

the constraint of locality preserving by allowing exponential tails in the definition of a local operator. We conjecture that there exist k -local circuits also for such *approximately locality-preserving unitaries* [92], as would be realized by Hamiltonian time evolution. As a concrete application, we expect that invertible chiral states (such as integer quantum Hall states) can be trivialized by k -local Hamiltonians, with use of constructions similar to the ones presented herein, although since we expect that chiral phases cannot be captured by zero-correlation-length models, there may not be a nicely behaved truncation to k -local circuits. Investigations of approximately locality-preserving unitaries would also connect to for example, the literature on state preparation with long-range Hamiltonians [93]. Lastly, we can consider a k -locality-preserving unitary (QCA $_k$) that maps local operators to k -local operators acting on at most k qubits. While we have shown that every QCA is an FDQC $_k$, this may not be true for QCA $_k$.

ACKNOWLEDGMENTS

We thank Daniel Bulmash, Tyler Ellison, Mike Hermele, and Dominic Williamson for discussions. We thank

Jeongwan Haah, Tyler Ellison, Drew Potter, and Carolyn Zhang for their feedback on the manuscript. Work by R.N. was supported by the U.S. Department of Energy, Office of Science, Basic Energy Sciences under Award No. DE-SC0021346. This work was begun during a visit to the Aspen Center for Physics (D.T.S., A.D., and R.N.). The Aspen Center for Physics is supported by the U.S. National Science Foundation (Grant No. PHY-1607611). A.D. and D.T.S. are supported by the Simons Foundation through the Simons Collaboration on Ultra-Quantum Matter [Grants No. 651440 (D.T.S.) and No. 651438 (A.D.)]. A.D. is supported by the Institute for Quantum Information and Matter, a National Science Foundation Physics Frontiers Center (Grant No. PHY-1733907). A.D., A.L., and R.N. acknowledge the Quantum Many-Body Dynamics and Noisy Intermediate-Scale Quantum Systems program of the Kavli Institute for Theoretical Physics, where part of the work was completed. The Kavli Institute for Theoretical Physics is supported by the National Science Foundation under Grant No. PHY-1748958. The authors acknowledge the University of Maryland for the supercomputing resources made available for conducting the research reported in this paper.

APPENDIX A: FINITE-TIME PROTOCOLS

In this appendix, we discuss k -local protocols that are not strictly of finite depth but that can nonetheless be generated in finite time by a k -local Hamiltonian. The advantage of the circuits constructed here is that all interactions are geometrically local, except for one special qubit, which can interact with every other qubit. That is, we add in a “one-to-all” interaction. While the special qubit is involved in the circuit used to create the SPT state, at the end of the circuit it remains decoupled from the rest of the spins. This can be viewed as modeling the scenario of a central spin problem, or a cavity QED setup in which atoms in a cavity all couple to a cavity mode. As a trade-off, these circuits are no longer of finite depth, but they can nonetheless be implemented via the finite-time evolution of a symmetric k -local Hamiltonian.

As a first example, we again consider the 1D cluster state $|\psi_C\rangle$. Suppose we have an even number N of qubits on a ring indexed as $i = 1, \dots, N$, plus an additional qubit indexed by $i = 0$ which lives in the middle of the ring. Suppose in addition that this qubit transforms under the symmetry as an even qubit, so that $X_{\text{even}} = \prod_{i=0}^{N/2} X_{2i}$, and consider the initial state $|\psi_C\rangle \otimes |+\rangle_0$. Then the following k -local gates are symmetric:

$$V_i = CZ_{0,2i-1}CZ_{2i-1,2i}CZ_{2i,2i+1}CZ_{2i+1,0}. \quad (\text{A1})$$

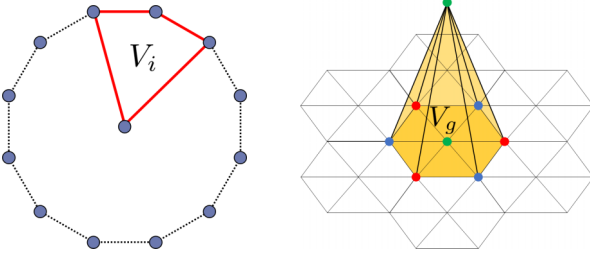


FIG. 9. Left: One gate in the one-to-all circuit for preparing the 1D cluster state, where each solid line represents a CZ gate. Right: One gate in the one-to-all circuit for the 2D hypergraph state where each colored triangular face represents a CCZ gate. In both cases, the product of all gates results in all unitaries involving the special qubit canceling pairwise.

This gate is pictured in Fig. 9. Then we have

$$\left(\prod_{i=1}^{N/2} V_i \right) |\psi_C\rangle \otimes |+\rangle_0 = |+\rangle^{\otimes N} \otimes |+\rangle_0, \quad (\text{A2})$$

so this disentangles the cluster state. Although there is intermediate entanglement between the central qubit and the ring, in the end, the central qubit remains in a product state. This circuit is not strictly of finite depth since every gate acts on the central qubit 0, so if we require layers to have nonoverlapping gates, it would require a linear number of layers. However, since all gates commute, they can be applied in finite time.

The same procedure works for 2D SPT states. Consider again the hypergraph state $|\psi_H\rangle$ on a closed 2D surface. We again add a special qubit 0, which we assume transforms like a qubit on a green-colored site. Let G denote the set of all green qubits on the 2D surface (not including the special qubit). Then, for every $g \in G$, let g_j for $j = 1, \dots, 6$ denote the six qubits neighboring g , which alternate between red and blue. Then define the k -local symmetric gates,

$$V_g = \prod_{j=1}^6 \text{CCZ}_{g, g_j, g_{j+1}} \text{CCZ}_{0, g_j, g_{j+1}}. \quad (\text{A3})$$

The gate is pictured in Fig. 9. Then we have

$$\left(\prod_{g \in G} V_g \right) |\psi_H\rangle \otimes |+\rangle_0 = |+\rangle^{\otimes N} \otimes |+\rangle_0. \quad (\text{A4})$$

This argument extends to all cocycle states in all dimensions as before. In all cases, it is important that the special qubit transforms in a certain way under the symmetry. If the symmetry did not act on the special qubit, the k -local gates we defined would not be symmetric.

This construction can be understood in terms of the path integral representation of SPT order. By viewing the spatial manifold on which the SPT state is defined as the boundary of some space-time in one higher dimension, one can construct the SPT state on the boundary using a product of local symmetric gates in the bulk [7]. The circuits we described are exactly of this form, where the bulk consists of a single ancillary qubit that couples to all qubits on the boundary. These same ideas have been used to define quantum pumps that pump a d -dimensional SPT state from a $(d+1)$ -dimensional bulk to the boundary. Such pumps have been constructed for general SPT states [94–97] and consist of symmetric gates in the bulk.

We remark that the notion of finite-time preparation is likely too powerful when it comes to the classification of phases. Indeed, any stabilizer state such as the GHZ state and the toric code ground state is equivalent to a graph state up to local unitaries [98]. A graph state is any state that can be prepared from a product state of all $|+\rangle$ states with use of CZ gates between pairs of qubits. Since all of these CZ gates commute, the graph state can be prepared in finite time with use of an Ising-type Hamiltonian. However, an important caveat is that in the case of the graph states that are equivalent to the GHZ and toric code states, there are qubits that must interact with a number of other qubits that is extensive in linear system size [42], which is somewhat unphysical. For example, if we were to impose the physical constraint that the total strength of interactions involving any one qubit is finite in the thermodynamic limit, i.e., a finite energy density, we must scale down the interaction strength of each Ising term accordingly. This has the consequence of requiring an interaction time that grows as the linear system size, which is consistent with the linear circuit depth. Conversely, if we do not scale the interactions down in this way, then we do not have a sensible thermodynamic limit—the energy density diverges as we make the system size large, indicating that our effective low-energy description in terms of an Ising Hamiltonian ceases to be a good approximation.

APPENDIX B: EXAMPLES OF k -LOCAL CIRCUITS FOR QCA

In this appendix, we illustrate our general construction of FDQC $_k$ s for QCA with a number of examples.

1. One-dimensional shift QCA

The 1D shift QCA that translates all sites to the right by one can be represented in the standard form with $d = 2$, $\ell = 1$, and $r = 4$. The u and v operators are defined as

$$u = \sum_{ij} |ij\rangle \langle i| \otimes |j\rangle \quad (\text{B1})$$

and

$$v = \sum_{ij} (|i\rangle \otimes |j\rangle) \langle ij|, \quad (\text{B2})$$

where u maps from a pair of 2D Hilbert spaces each spanned by the states $|0\rangle$ and $|1\rangle$ into a 4D Hilbert space spanned by $|00\rangle$, $|01\rangle$, $|10\rangle$, and $|11\rangle$, and similarly for v . Graphically, we can draw these operators as follows:

$$u = \begin{array}{c} \text{---} \\ \text{---} \\ \text{---} \\ \text{---} \end{array}, \quad v = \begin{array}{c} \text{---} \\ \text{---} \\ \text{---} \\ \text{---} \end{array}. \quad (\text{B3})$$

One can see how these operators implement the shift QCA by drawing the whole circuit:

$$Q = \dots \begin{array}{c} \text{---} \\ \text{---} \\ \text{---} \\ \text{---} \end{array} \dots \quad (\text{B4})$$

Following the lines, one can clearly see that every site is translated to the right by one.

The spatial inversions of u and v are obtained by swapping the left and right input and output Hilbert spaces, giving $\bar{u} = \sum_{ij} |ij\rangle \langle j| \otimes \langle i|$ and $\bar{v} = \sum_{ij} (|j\rangle \otimes |i\rangle) \langle ij|$. From this, we compute

$$w = \bar{v}u = \sum_{ij} (|j\rangle \otimes |i\rangle) \langle i| \otimes \langle j| = \text{SWAP} \quad (\text{B5})$$

and $\bar{w} = w$. Next, note that the circuit V_R defined in Eq. (12) consists of two types of gate, the simple SWAP gate S_i and the gate $V_i = Q_A^{-1} S_i Q_A$, which in the present case is also a SWAP gate.

Finally, we apply the gates S_i , V_i , and w , which are all SWAP gates, in the order described by Eq. (19). This gives a depth-4 FDQC_k composed of 2-local SWAP gates realizing the shift QCA, as shown in Fig. 10. The resulting FDQC_k is similar to that shown in Fig. 4, although somewhat more complicated as a consequence of the more general construction it comes from.

2. One-dimensional cluster state

As discussed in Sec. IV C, we can also apply our construction to the FDQC s that create SPT fixed-point states. We illustrate this for the simple example of the 1D cluster state. The FDQC that constructs the 1D cluster state is given in Eq. (2). Observe that this circuit commutes with the $\mathbb{Z}_2 \times \mathbb{Z}_2$ symmetry generated by X_{odd} and X_{even} as a whole, but the individual gates that compose the circuit do not commute with the symmetry. Therefore, this is not a symmetric FDQC . We can apply our general construction with $Q = \prod_i \text{CZ}_{i,i+1}$ to obtain a symmetric FDQC_k that implements the same operator.

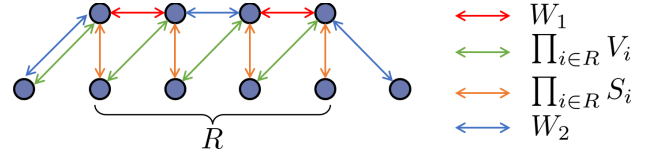


FIG. 10. FDQC_k for the 1D shift QCA resulting from the general construction in Sec. IV. The lower (upper) row of sites belongs to the system A (B). The SWAP gates are applied in the order red, green, yellow, and blue, which have the combined effect of shifting all sites by one counterclockwise. Notice the similar trapezoidal arrangement of sites compared with the general structure shown in Fig. 5.

The operators u and v are both equal to the CZ operator. Note that the CZ gate is symmetric under spatial inversion. Then we have $w = I$, and the FDQC_k is simply given by V_R [Eq. (12)]. As before, V_R is composed of SWAP gates S_i and the gates V_i . The latter is equal to the gate

$$V_i = \begin{array}{c} \bullet \\ \text{---} \\ \bullet \end{array} \quad (\text{B6})$$

where the lower (upper) row of qubits belongs to the system A (B), and the four CZ gates (red lines) act before the SWAP gate (arrow). This particular product of CZ gates commutes with the $\mathbb{Z}_2 \times \mathbb{Z}_2$ symmetry, as do the SWAP gates $\text{CZ}S_i$. It is straightforward to check that $V_R = (\prod_{i \in R} S_i)(\prod_{i \in R} V_i)$ is equal to the operator.

$$\begin{array}{c} \bullet \text{---} \bullet \text{---} \bullet \text{---} \bullet \\ \text{---} \\ \bullet \text{---} \bullet \text{---} \bullet \text{---} \bullet \end{array} \quad (\text{B7})$$

which is exactly Q applied to a finite ring. Therefore, this gives an alternative construction for a symmetric FDQC_k realizing the 1D cluster state that is similar to, but distinct from, the circuit in Eq. (4).

3. Two-dimensional diagonal-shift QCA

Here we show how our construction applies to higher-dimensional QCA by considering the 2D diagonal-shift QCA that translates all sites up and to the right by one site. This example highlights the need for the inductive part of the proof, where we decompose the QCA into products of lower-dimensional QCA until an FDQC_k is created.

We consider implementing the operation on a 2D torus of size $L_x \times L_y$. As described in Sec. IV B, we first compactify the lattice along the y direction and write the QCA in the standard form. This requires $d = 2^{L_y}$, $\ell = 1$, and

$r = 2^{2L_y}$. Then we have

$$u = \sum_{\vec{i}, \vec{j}} |s(\vec{i})\vec{j}\rangle \langle (\vec{i} | \otimes \langle \vec{j} |) \quad (\text{B8})$$

and

$$v = \sum_{\vec{i}, \vec{j}} \langle (\vec{i} | \otimes |s(\vec{j})\rangle) \langle \vec{j} |, \quad (\text{B9})$$

where $\vec{i} = (i_1, \dots, i_{L_y})$ and $s(\vec{i}) = (i_{L_y}, i_1, \dots, i_{L_y-1})$ is a vertical translation of \vec{i} . The spatial inversions \vec{u} and \vec{v} are defined as in the case of the 1D shift QCA. We then calculate

$$\begin{aligned} w &= \sum_{\vec{i}, \vec{j}} (|s(\vec{j})\rangle \otimes |s(\vec{i})\rangle) \langle (\vec{i} | \otimes \langle \vec{j} |) \\ &= (\text{SHIFT}_y \otimes \text{SHIFT}_y) \overrightarrow{\text{SWAP}} \end{aligned} \quad (\text{B10})$$

where $\overrightarrow{\text{SWAP}}$ swaps the two columns indexed by \vec{i} and \vec{j} , and SHIFT_y translates all sites in a column up by one. We observe here that w is composed of lower-dimensional QCA, and is not an FDQC itself. This illustrates the need for the inductive part of the proof. We can express w as an FDQC $_k$ as shown in Sec. B 1.

To obtain the complete FDQC $_k$ realizing the diagonal-shift QCA, we combine V_R , which is just a sequence of two products of pairwise SWAP operations between sites, with products of w and \bar{w} as described in Eq. (19).

APPENDIX C: PROPERTIES OF THE OPERATOR w

The following lemma is used in Sec. IV to show that the operator w is locality preserving.

Lemma 1.—Consider a system of qubits divided into regions A and $B = \bar{A}$. Let O be an operator acting on the whole system. Using Schmidt decomposition, one can always write O as

$$O = \sum_{k=1}^M A_k \otimes B_k \quad (\text{C1})$$

such that A_k and B_k are operators acting on regions A and B , respectively, and all A_k operators are linearly independent and all B_k operators are also linearly independent. Assume O acts trivially on a qubit j . Then, if O is written as above, each A_k and each B_k should act trivially on qubit j as well.

Proof.—Without loss of generality, we assume $j \in A$, from which it trivially follows that B_k operators act as the identity on j . Let P_j be an arbitrary operator supported on

qubit j . Since O acts trivially on j , we have $[O, P_j] = 0$ and thus

$$\sum_{k=1}^M [A_k, P_j] \otimes B_k = 0. \quad (\text{C2})$$

Let $|\psi\rangle$ be an arbitrary state in the region A . If we multiply both sides of the above equality by $|\psi\rangle\langle\psi| \otimes \mathbb{I}_B$ and trace over A , we get

$$\sum_{k=1}^M \langle\psi|[A_k, P_j]|\psi\rangle B_k = 0. \quad (\text{C3})$$

Since B_k operators are linearly independent, we find that $\langle\psi|[A_k, P_j]|\psi\rangle = 0$ for all k . Since $|\psi\rangle$ was arbitrary, it follows that $[A_k, P_j] = 0$. Finally, since P_j was arbitrary, we conclude that A_k should act trivially on qubit j . ■

In the following lemma, we show that the unitary w defined in Sec. IV commutes with all global symmetries of Q .

Lemma 2.—If $[Q, S] = 0$, where $S = s^{\otimes N}$, then $[w, S] = 0$.

Proof.—Recall the Margolus representation of Q in Eq. (13), which defines Q in terms of the matrices u and v . If $[Q, S] = 0$, then $S^{-1}QS = Q$, so $u' = u(s \otimes s)$ and $v' = (s^{-1} \otimes s^{-1})v$ define the same QCA as u and v . Then, by Theorem 3.10 in Ref. [64], there must exist unitaries x and y such that $u' = (x \otimes y)u$ and $v' = v(y^{-1} \otimes x^{-1})$ [note that Eq. (35b) in Ref. [64] implies the condition on v via Eq. (29b) therein]. Defining $w' = \bar{v}'u'$, we have

$$w' = \bar{v}(x^{-1} \otimes y^{-1})(x \otimes y)u = \bar{v}u \equiv w,$$

so

$$w' \equiv (s^{-1} \otimes s^{-1})w(s \otimes s) = w,$$

which gives $[w, S] = 0$. ■

Lastly, in the following lemma, we argue that if Q is transitionally invariant in the compactified direction, then w is also transitionally invariant in the compactified direction.

Lemma 3.—If T is a translation along the compactified directions, then for any operator O supported on supersites $2i$ and $2i + 1$, we have $wTOT^\dagger w^\dagger = TwOw^\dagger T^\dagger$.

Proof.—Let O be an operator supported on supersites $2i$ and $2i + 1$. Let $uOu^{-1} = \sum_k A^k \otimes B^k$, where A^k (B^k) are linearly independent operators supported on the l -dimensional (r -dimensional) Hilbert space that comes out of u . We also define $C^k = vA^k v^{-1}$ and $D^k = vB^k v^{-1}$. On the other hand, let $u(\text{TOT}^\dagger)u^{-1} = \sum_k \tilde{A}^k \otimes \tilde{B}^k$, where \tilde{A}^k (\tilde{B}^k) are linearly independent operators supported on the l -dimensional (r -dimensional) Hilbert spaces. We also define $\tilde{C}^k = v\tilde{A}^k v^{-1}$ and $\tilde{D}^k = v\tilde{B}^k v^{-1}$. Note that $QOQ^{-1} = \sum_k C^k \otimes D^k$, where C^k operators act on supersites $2i - 1$ and $2i$ and D^k acts on supersites $2i + 1$

and $2i + 2$. On the other hand, we have $Q(\text{TOT}^\dagger)Q^{-1} = \sum_k \tilde{C}^k \otimes \tilde{D}^k$. Since Q is translationally invariant, we have

$$\sum_k \tilde{C}^k \otimes \tilde{D}^k = \sum_k TC^k T^\dagger \otimes TD^k T^\dagger. \quad (\text{C4})$$

When we act on TOT^\dagger with w we get,

$$w(\text{TOT}^\dagger)w^\dagger = \sum_k \widetilde{C^k D^k} = \text{SWAP} \left[\sum_k \tilde{C}^k \tilde{D}^k \right], \text{swap}, \quad (\text{C5})$$

where SWAP exchanges the two supersites on which w acts. However, it follows from Eq. (C4) that $\sum_k \tilde{C}^k \tilde{D}^k = \sum_k TC^k D^k T^\dagger$, which is easy to see graphically:

$$\sum_k \begin{array}{c} \rho \quad \sigma \\ \text{---} \\ \text{---} \\ \mu \quad \nu \end{array} = \text{Tr}_{\alpha, \gamma} \left[\text{Tr}_{\beta, \delta} \left[\sum_k \begin{array}{c} \rho \quad \sigma \quad \gamma \quad \delta \\ \text{---} \\ \text{---} \\ \alpha \quad \beta \quad \mu \quad \nu \end{array} \right] \right]$$

$$= \text{Tr}_{\alpha, \gamma} \left[\text{Tr}_{\beta, \delta} \left[\sum_k \begin{array}{c} \rho \quad \sigma \quad \gamma \quad \delta \\ \text{---} \\ \text{---} \\ \alpha \quad \beta \quad \mu \quad \nu \end{array} \right] \right]$$

$$= \sum_k \begin{array}{c} \rho \quad \sigma \\ \text{---} \\ \text{---} \\ \mu \quad \nu \end{array} \quad (\text{C6})$$

where $\text{Tr}_{\alpha, \beta}$ means contracting the α and β indices. In the first line, we have used the linearity of the trace to move the sum over k inside the trace. To go to the second line, we used Eq. (C4), and the third line follows by our moving the sum outside the traces and contracting the relevant indices. Lastly, since the SWAP operation between supersites commutes with the translation T along

the compactified directions, we find that

$$\begin{aligned} w(\text{TOT}^\dagger)w^\dagger &= \text{SWAP} T \left[\sum_k C^k D^k \right] T \text{SWAP} \\ &= T \left[\sum_k \widetilde{C^k D^k} \right] T \\ &= T w O w^\dagger T^\dagger. \end{aligned} \quad (\text{C7})$$

■

APPENDIX D: LIGHT CONE ARGUMENT FOR k -LOCAL NONTRIVIALITY

In this appendix, we briefly review the proof for k -local nontriviality of code states of quantum error correcting codes. The argument is basically the same as the light cone argument presented in Ref. [8], which was used to show that topological states on manifolds of nonzero genus cannot be prepared by constant-depth local unitaries but can be prepared with the slight modification of replacing locality with k locality.

Let $|\psi_1\rangle$ and $|\psi_2\rangle$ be two orthogonal code states of an N -qubit quantum code. Furthermore, assume the corresponding quantum error correcting code has distance d , so for any operator that acts on fewer than d qubits we have

$$\langle \psi_1 | O | \psi_1 \rangle = \langle \psi_2 | O | \psi_2 \rangle. \quad (\text{D1})$$

Let U be a k -local circuit that prepares $|\psi_1\rangle$ in depth D , starting from the trivial state $|0\rangle^{\otimes N}$:

$$|\psi_1\rangle = U|0\rangle^{\otimes N}. \quad (\text{D2})$$

In the following, we show that $D \geq \log_k(d)$. Assume that is not true, meaning that $D < \log_k(d)$. Let $\pi_j = |0\rangle\langle 0|_j$ denote the projection operator that projects the j th qubit into the $|0\rangle$ state. Note that π_j has support only on qubit j . Since U is a k -local circuit of depth D , the operator $U\pi_j U^\dagger$ can have nontrivial support on at most k^D qubits, which is less than d [because of the assumption $D < \log_k(d)$]. Therefore, due to Eq. (D1) we have

$$\langle \psi_2 | U\pi_j U^\dagger | \psi_2 \rangle = \langle \psi_1 | U\pi_j U^\dagger | \psi_1 \rangle = 1, \quad (\text{D3})$$

where we have used Eq. (D2) in the last step. Since j was arbitrary, we should have $U^\dagger |\psi_2\rangle = e^{i\theta} |0\rangle^{\otimes N}$, for some phase θ , or equivalently $|\psi_2\rangle = e^{i\theta} |\psi_1\rangle$. But this contradicts the assumption that $|\psi_1\rangle$ and $|\psi_2\rangle$ are orthogonal code states; hence, $D \geq \log_k(d)$.

The above argument shows that the code states of quantum error correcting codes with a nonzero number of logical qubits, whose distance goes to infinity in the thermodynamic limit, are k -local nontrivial, meaning that they

cannot be prepared by a k -local constant-depth unitary circuit. This includes, for example, the ground states of the toric code on a torus. However, the argument above says nothing about the complexity of preparing the ground state of the topological Hamiltonians such as the toric code on a sphere that has genus zero, because in this case the ground state is unique (so there is no other orthogonal ground state $|\psi_2\rangle$). Similarly, the light cone argument does not work for SPT states on closed manifolds since the ground state of an SPT Hamiltonian on a closed manifold is unique. While a more involved argument [33] shows that topological states on zero-genus surfaces are still k -local nontrivial, our result shows that SPT states in contrast are all k -local trivial. It is worth noting that although SPT phases on manifolds with open boundary conditions have degenerate ground states, the light cone argument is still inapplicable. This is because although Eq. (D1) holds for symmetric local operators, it can be violated by symmetric but k -local operators.

APPENDIX E: MORE DETAILS ON THE NUMERICAL STUDY OF SPT ORDER IN MONITORED RANDOM CIRCUITS

In this appendix, we provide additional details about the transitions that were discussed in Sec. V A. The order parameter that we used to probe the late-time states was given as

$$s = \frac{2}{N(N-1)} \sum_{a < b} S(a, b)^2, \quad (\text{E1})$$

with $S(a, b)$ denoting the string order parameter defined in Eq. (22). A state in the SPT phase is characterized by a finite nonzero value of $S(a, b)$ for sufficiently far apart a and b . In this case, the sum in Eq. (E1) is dominated by sites a and b that are $O(N)$ far apart, and since there are $O(N^2)$ such (a, b) pairs, one expects that the parameter s goes to some finite nonzero value in the thermodynamic limit. On the other hand, for a trivial state, $S(a, b)$ goes to zero exponentially fast, so only the local terms with $b - a$ smaller than the correlation length contribute to the sum in Eq. (E1), and since there are $O(N)$ such terms, one expects s to drop as $1/N$ for large N and to go to 0 in the thermodynamic limit. This scaling can be seen in our setup as expected. Figure 11 shows the order parameter s as a function of N for fixed $p = 0.1$, with both axes scaling logarithmically. Note that s vanishes as $1/N$ for large N in Figs. 11(a) and 11(c), which correspond to local (but not necessarily symmetric) two-qubit unitaries and 2-local symmetric unitaries, respectively, while it saturates to a finite nonzero value in Figs. 11(b) and 11(d), which correspond to local symmetric two-qubit unitaries and 2-local ‘‘locally’’ symmetric unitaries (see Sec. V A), respectively.

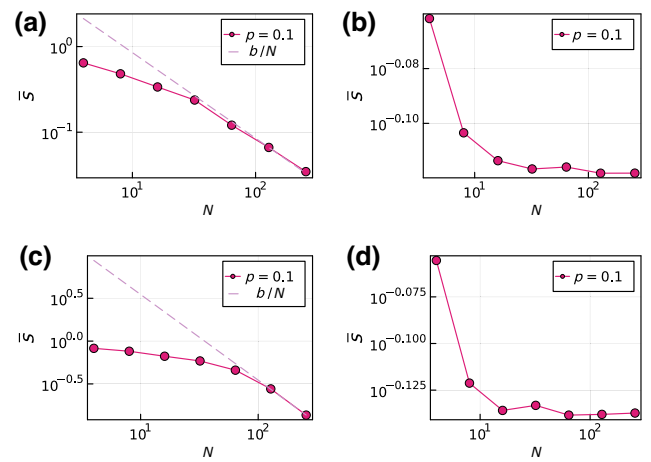


FIG. 11. Average string order parameter \bar{s} versus N at fixed $p = 0.1$ in the late-time states of monitored random circuits described in Sec. V A where the unitary gates are chosen randomly from (a) local two-qubit Clifford unitaries, (b) local two-qubit $\mathbb{Z}_2 \times \mathbb{Z}_2$ symmetric Clifford unitaries, (c) 2-local $\mathbb{Z}_2 \times \mathbb{Z}_2$ symmetric Clifford unitaries, and (d) 2-local \mathbb{Z}_2^N symmetric Clifford unitaries.

Moreover, for monitored circuits where the SPT order survives up to nonzero values of p , i.e., for local symmetric unitaries and 2-local unitaries that are locally symmetric [Figs. 11(b) and 11(d)], one can study the phase transition at p_c by using data collapse for finite-size systems. Following Ref. [72], we assume the form

$$s(p, N) - s(p_c, N) = N^{-1} F[(p - p_c) N^{1/\nu}], \quad (\text{E2})$$

near the critical point, where p_c is the critical value for applying unitary gates and ν is the correlation length critical exponent, and we can search for values of p_c and ν that result in the best data collapse. Figure 12 shows the best collapse with use of the data points shown in Fig. 7, giving $p_c = 0.50(5)$ for both local symmetric gates as well as 2-local locally symmetric gates. On the other hand, the correlation length critical exponents ν for local symmetric gates and 2-local locally symmetric gates are 1.3(2) and

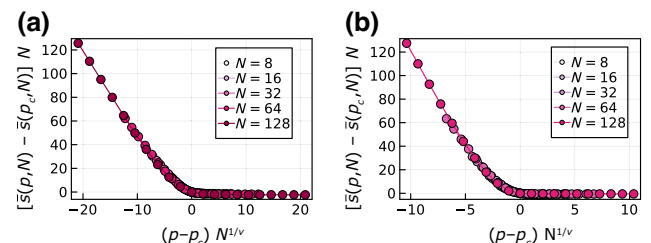


FIG. 12. Data collapse of data points shown in Fig. 7 for (a) when gates are chosen to be local symmetric Clifford gates with $p_c = 0.50(5)$ and $\nu = 1.3(2)$ and (b) when gates are chosen to be 2-local locally symmetric Clifford gates with $p_c = 0.50(5)$ and $\nu = 1.6(1)$.

1.6(1), respectively. In principle one needs to get more data near the critical point and use them for data collapse to get better estimates of p_c and ν .

-
- [1] Xiao-Gang Wen, *Quantum Field Theory of Many-Body Systems: From the Origin of Sound to an Origin of Light and Electrons* (Oxford University Press on Demand, Oxford, 2004).
- [2] Xiao-Gang Wen, Colloquium: Zoo of quantum-topological phases of matter, *Rev. Mod. Phys.* **89**, 041004 (2017).
- [3] Héctor Bombín, An introduction to topological quantum codes, *ArXiv:1311.0277* (2013).
- [4] Ville Lahtinen and Jiannis K. Pachos, A short introduction to topological quantum computation, *SciPost Phys.* **3**, 021 (2017).
- [5] Xie Chen, Zheng-Cheng Gu, and Xiao-Gang Wen, Local unitary transformation, long-range quantum entanglement, wave function renormalization, and topological order, *Phys. Rev. B* **82**, 155138 (2010).
- [6] T. Senthil, Symmetry-protected topological phases of quantum matter, *Annu. Rev. Condens. Matter Phys.* **6**, 299 (2015).
- [7] Xie Chen, Zheng-Cheng Gu, Zheng-Xin Liu, and Xiao-Gang Wen, Symmetry protected topological orders and the group cohomology of their symmetry group, *Phys. Rev. B* **87**, 155114 (2013).
- [8] S. Bravyi, M. B. Hastings, and F. Verstraete, Lieb-Robinson bounds and the generation of correlations and topological quantum order, *Phys. Rev. Lett.* **97**, 050401 (2006).
- [9] Nathanan Tantivasadakarn, Ashvin Vishwanath, and Ruben Verresen, A hierarchy of topological order from finite-depth unitaries, measurement and feedforward, *ArXiv:2209.06202* (2022).
- [10] Lorenzo Piroli, Georgios Styliaris, and J. Ignacio Cirac, Quantum circuits assisted by local operations and classical communication: Transformations and phases of matter, *Phys. Rev. Lett.* **127**, 220503 (2021).
- [11] Sergey Bravyi, Isaac Kim, Alexander Kliesch, and Robert Koenig, Adaptive constant-depth circuits for manipulating non-abelian anyons, *ArXiv:2205.01933* (2022).
- [12] Yichen Huang and Xie Chen, Quantum circuit complexity of one-dimensional topological phases, *Phys. Rev. B* **91**, 195143 (2015).
- [13] Yu-Jie Liu, Kirill Shtengel, Adam Smith, and Frank Pollmann, Methods for simulating string-net states and anyons on a digital quantum computer, *PRX Quantum* **3**, 040315 (2022).
- [14] Zongyuan Wang, Xiuqi Ma, David T. Stephen, Michael Hermele, and Xie Chen, Renormalization of Ising cage-net model and generalized foliation (to be published).
- [15] Ehud Altman, *et al.*, Quantum simulators: Architectures and opportunities, *PRX Quantum* **2**, 017003 (2021).
- [16] G. Semeghini, H. Levine, A. Keesling, S. Ebadi, T. T. Wang, D. Bluvstein, R. Verresen, H. Pichler, M. Kalinowski, R. Samajdar, A. Omran, S. Sachdev, A. Vishwanath, M. Greiner, V. Vuletić, and M. D. Lukin, Probing topological spin liquids on a programmable quantum simulator, *Science* **374**, 1242 (2021).
- [17] J. F. Marques, B. M. Varbanov, M. S. Moreira, H. Ali, N. Muthusubramanian, C. Zachariadis, F. Battistel, M. Beekman, N. Haider, W. Vlothuizen, A. Bruno, B. M. Terhal, and L. DiCarlo, Logical-qubit operations in an error-detecting surface code, *Nat. Phys.* **18**, 80 (2022).
- [18] Austin G. Fowler and John M. Martinis, Quantifying the effects of local many-qubit errors and nonlocal two-qubit errors on the surface code, *Phys. Rev. A* **89**, 032316 (2014).
- [19] Philip Richerme, Zhe-Xuan Gong, Aaron Lee, Crystal Senko, Jacob Smith, Michael Foss-Feig, Spyridon Michalakis, Alexey V. Gorshkov, and Christopher Monroe, Non-local propagation of correlations in quantum systems with long-range interactions, *Nature* **511**, 198 (2014).
- [20] Varun D. Vaidya, Yudan Guo, Ronen M. Kroeze, Kyle E. Ballantine, Alicia J. Kollár, Jonathan Keeling, and Benjamin L. Lev, Tunable-range, photon-mediated atomic interactions in multimode cavity QED, *Phys. Rev. X* **8**, 011002 (2018).
- [21] J. Eli Bourassa, Rafael N. Alexander, Michael Vasmer, Ashlesha Patil, Ilan Tzitrin, Takaya Matsuura, Daiqin Su, Ben Q. Baragiola, Saikat Guha, Guillaume Dauphinais, Krishna K. Sabapathy, Nicolas C. Menicucci, and Ish Dhand, Blueprint for a scalable photonic fault-tolerant quantum computer, *Quantum* **5**, 392 (2021).
- [22] Terry Farrelly, A review of quantum cellular automata, *Quantum* **4**, 368 (2020).
- [23] D. Gross, V. Nesme, H. Vogts, and R. F. Werner, Index theory of one dimensional quantum walks and cellular automata, *Commun. Math. Phys.* **310**, 419 (2012).
- [24] Michael Freedman and Matthew B. Hastings, Classification of quantum cellular automata, *Commun. Math. Phys.* **376**, 1171 (2020).
- [25] Jeongwan Haah, Lukasz Fidkowski, and Matthew B. Hastings, Nontrivial quantum cellular automata in higher dimensions, *Commun. Math. Phys.* **398**, 469 (2022).
- [26] Jeongwan Haah, Clifford quantum cellular automata: Trivial group in 2D and Witt group in 3D, *J. Math. Phys.* **62**, 092202 (2021).
- [27] Wilbur Shirley, Yu-An Chen, Arpit Dua, Tyler D. Ellison, Nathanan Tantivasadakarn, and Dominic J. Williamson, Three-dimensional quantum cellular automata from chiral semion surface topological order and beyond, *PRX Quantum* **3**, 030326 (2022).
- [28] David T. Stephen, Hendrik Poulsen Nautrup, Juani Bermejo-Vega, Jens Eisert, and Robert Raussendorf, Subsystem symmetries, quantum cellular automata, and computational phases of quantum matter, *Quantum* **3**, 142 (2019).
- [29] Lukasz Fidkowski, Jeongwan Haah, and Matthew B. Hastings, Exactly solvable model for a 4 + 1D beyond-cohomology symmetry-protected topological phase, *Phys. Rev. B* **101**, 155124 (2020).
- [30] Hoi Chun Po, Lukasz Fidkowski, Takahiro Morimoto, Andrew C. Potter, and Ashvin Vishwanath, Chiral Floquet phases of many-body localized bosons, *Phys. Rev. X* **6**, 041070 (2016).

- [31] Lukasz Fidkowski, Hoi Chun Po, Andrew C. Potter, and Ashvin Vishwanath, Interacting invariants for Floquet phases of fermions in two dimensions, *Phys. Rev. B* **99**, 085115 (2019).
- [32] Hoi Chun Po, Lukasz Fidkowski, Ashvin Vishwanath, and Andrew C. Potter, Radical chiral Floquet phases in a periodically driven Kitaev model and beyond, *Phys. Rev. B* **96**, 245116 (2017).
- [33] Dorit Aharonov and Yonathan Touati, Quantum circuit depth lower bounds for homological codes, *ArXiv:1810.03912* (2018).
- [34] Daniel Azses, Rafael Haenel, Yehuda Naveh, Robert Raussendorf, Eran Sela, and Emanuele G. Dalla Torre, Identification of symmetry-protected topological states on noisy quantum computers, *Phys. Rev. Lett.* **125**, 120502 (2020).
- [35] Xiao Xiao, J. K. Freericks, and A. F. Kemper, Determining quantum phase diagrams of topological Kitaev-inspired models on NISQ quantum hardware, *Quantum* **5**, 553 (2021).
- [36] G. Semeghini, H. Levine, A. Keesling, S. Ebadi, T. T. Wang, D. Bluvstein, R. Verresen, H. Pichler, M. Kalinowski, R. Samajdar, A. Omran, S. Sachdev, A. Vishwanath, M. Greiner, V. Vuletić, and M. D. Lukin, Probing topological spin liquids on a programmable quantum simulator, *Science* **374**, 1242 (2021).
- [37] Adam Smith, Bernhard Jobst, Andrew G. Green, and Frank Pollmann, Crossing a topological phase transition with a quantum computer, *Phys. Rev. Res.* **4**, L022020 (2022).
- [38] Tsung-Cheng Lu, Leonardo A. Lessa, Isaac H. Kim, and Timothy H. Hsieh, Measurement as a shortcut to long-range entangled quantum matter, *PRX Quantum* **3**, 040337 (2022).
- [39] Xiao Mi, *et al.*, Time-crystalline eigenstate order on a quantum processor, *Nature* **601**, 531 (2022).
- [40] Philipp T. Dumitrescu, Justin G. Bohnet, John P. Gaebler, Aaron Hankin, David Hayes, Ajesh Kumar, Brian Neyenhuis, Romain Vasseur, and Andrew C. Potter, Dynamical topological phase realized in a trapped-ion quantum simulator, *Nature* **607**, 463 (2022).
- [41] Diogo Cruz, Romain Fournier, Fabien Gremion, Alix Jeanerot, Kenichi Komagata, Tara Tosić, Jarla Thiesbrummel, Chun Lam Chan, Nicolas Macris, Marc-André Dupertuis, and Clément Javerzac-Galy, Efficient quantum algorithms for GHZ and W states, and implementation on the IBM quantum computer, *Adv. Quantum Technol.* **2**, 1900015 (2019).
- [42] Pengcheng Liao and David L. Feder, Graph-state representation of the toric code, *Phys. Rev. A* **104**, 012432 (2021).
- [43] Robert König, Ben W. Reichardt, and Guifré Vidal, Exact entanglement renormalization for string-net models, *Phys. Rev. B* **79**, 195123 (2009).
- [44] Hans J. Briegel and Robert Raussendorf, Persistent entanglement in arrays of interacting particles, *Phys. Rev. Lett.* **86**, 910 (2001).
- [45] W. Son, L. Amico, and V. Vedral, Topological order in 1D cluster state protected by symmetry, *Quantum Inf. Process.* **11**, 1961 (2012).
- [46] Xie Chen, Zheng-Cheng Gu, and Xiao-Gang Wen, Classification of gapped symmetric phases in one-dimensional spin systems, *Phys. Rev. B* **83**, 035107 (2011).
- [47] Yang-Zhi Chou, Rahul M. Nandkishore, and Leo Radzihovskiy, Gapless insulating edges of dirty interacting topological insulators, *Phys. Rev. B* **98**, 054205 (2018).
- [48] Itamar Kimchi, Yang-Zhi Chou, Rahul M. Nandkishore, and Leo Radzihovskiy, Anomalous localization at the boundary of an interacting topological insulator, *Phys. Rev. B* **101**, 035131 (2020).
- [49] Beni Yoshida, Topological phases with generalized global symmetries, *Phys. Rev. B* **93**, 155131 (2016).
- [50] Michael Levin and Zheng-Cheng Gu, Braiding statistics approach to symmetry-protected topological phases, *Phys. Rev. B* **86**, 115109 (2012).
- [51] The Levin-Gu state can be obtained by acting on $|\psi_H\rangle$ with a CZ gate on every neighboring pair of spins and a Z gate on every spin [73].
- [52] Robert Raussendorf, Cihan Okay, Dong-Sheng Wang, David T. Stephen, and Hendrik Poulsen Nautrup, Computationally universal phase of quantum matter, *Phys. Rev. Lett.* **122**, 090501 (2019).
- [53] Yizhi You, Trithep Devakul, F. J. Burnell, and S. L. Sondhi, Subsystem symmetry protected topological order, *Phys. Rev. B* **98**, 035112 (2018).
- [54] Trithep Devakul, Yizhi You, F. J. Burnell, and S. L. Sondhi, Fractal symmetric phases of matter, *SciPost Phys.* **6**, 7 (2019).
- [55] Trithep Devakul, Dominic J. Williamson, and Yizhi You, Classification of subsystem symmetry-protected topological phases, *Phys. Rev. B* **98**, 235121 (2018).
- [56] Yizhi You, Trithep Devakul, F. J. Burnell, and S. L. Sondhi, Symmetric fracton matter: Twisted and enriched, *Ann. Phys. (N. Y.)* **416**, 168140 (2020).
- [57] Robert Raussendorf, Sergey Bravyi, and Jim Harrington, Long-range quantum entanglement in noisy cluster states, *Phys. Rev. A* **71**, 062313 (2005).
- [58] Sam Roberts and Stephen D. Bartlett, Symmetry-protected self-correcting quantum memories, *Phys. Rev. X* **10**, 031041 (2020).
- [59] Kevin Walker and Zhenghan Wang, (3+1)-TQFTs and topological insulators, *Front. Phys.* **7**, 150 (2012).
- [60] Pablo Arrighi, Vincent Nesme, and Reinhard Werner, Unitarity plus causality implies localizability, *J. Comput. Syst. Sci.* **77**, 372 (2011).
- [61] B. Schumacher and R. F. Werner, Reversible quantum cellular automata, *ArXiv:quant-ph/0405174* (2004).
- [62] Indeed, if we let $\text{ind}(Q)$ be the rational-valued index of Q as defined in Ref. [23], then it is straightforward to show that $\text{ind}(Q^{-1}) = \text{ind}(Q)^{-1} = \text{ind}(\bar{Q})$, which implies that Q^{-1} and \bar{Q} differ by an FDQC in one dimension [23].
- [63] Pablo Arrighi, Vincent Nesme, and Reinhard Werner, in *Language and Automata Theory and Applications*, edited by Carlos Martín-Vide, Friedrich Otto, and Henning Fernau (Springer, Berlin, 2008), p. 64.
- [64] J. Ignacio Cirac, David Perez-Garcia, Norbert Schuch, and Frank Verstraete, Matrix product unitaries: Structure, symmetries, and topological invariants, *J. Stat. Mech.: Theory Exp.* **2017**, 083105 (2017).

- [65] F. J. Burnell, Xie Chen, Lukasz Fidkowski, and Ashvin Vishwanath, Exactly soluble model of a three-dimensional symmetry-protected topological phase of bosons with surface topological order, *Phys. Rev. B* **90**, 245122 (2014).
- [66] Frank Pollmann and Ari M. Turner, Detection of symmetry-protected topological phases in one dimension, *Phys. Rev. B* **86**, 125441 (2012).
- [67] D. Pérez-García, M. M. Wolf, M. Sanz, F. Verstraete, and J. I. Cirac, String order and symmetries in quantum spin lattices, *Phys. Rev. Lett.* **100**, 167202 (2008).
- [68] Matthew P. A. Fisher, Vedika Khemani, Adam Nahum, and Sagar Vijay, Random quantum circuits, *ArXiv:2207.14280* (2022).
- [69] Ali Lavasani, Yahya Alavirad, and Maissam Barkeshli, Measurement-induced topological entanglement transitions in symmetric random quantum circuits, *Nat. Phys.* **17**, 342 (2021).
- [70] Aaron J. Friedman, Oliver Hart, and Rahul Nandkishore, Measurement-induced phases of matter require adaptive dynamics, *ArXiv:2210.07256* (2022).
- [71] Yasaman Bahri, Ronen Vosk, Ehud Altman, and Ashvin Vishwanath, Localization and topology protected quantum coherence at the edge of hot matter, *Nat. Commun.* **6**, 7341 (2015).
- [72] Shengqi Sang and Timothy H. Hsieh, Measurement-protected quantum phases, *Phys. Rev. Res.* **3**, 023200 (2021).
- [73] Tzu-Chieh Wei, Quantum spin models for measurement-based quantum computation, *Adv. Phys.: X* **3**, 1461026 (2018).
- [74] R. Raussendorf, J. Harrington, and K. Goyal, A fault-tolerant one-way quantum computer, *Ann. Phys. (N. Y.)* **321**, 2242 (2006).
- [75] Chong Wang and T. Senthil, Interacting fermionic topological insulators/superconductors in three dimensions, *Phys. Rev. B* **89**, 195124 (2014).
- [76] Lorenzo Piroli, Alex Turzillo, Sujeet K. Shukla, and J. Ignacio Cirac, Fermionic quantum cellular automata and generalized matrix-product unitaries, *J. Stat. Mech.: Theory Exp.* **2021**, 013107 (2021).
- [77] Maissam Barkeshli, Parsa Bonderson, Meng Cheng, and Zhenghan Wang, Symmetry fractionalization, defects, and gauging of topological phases, *Phys. Rev. B* **100**, 115147 (2019).
- [78] Rahul M. Nandkishore and Michael Hermele, Fractons, *Annu. Rev. Condens. Matter Phys.* **10**, 295 (2019).
- [79] Michael Pretko, Xie Chen, and Yizhi You, Fracton phases of matter, *Int. J. Mod. Phys. A* **35**, 2030003 (2020).
- [80] Andrey Gromov and Leo Radzihovsky, Fracton matter, *ArXiv:2211.05130* (2022).
- [81] Sagar Vijay, Jeongwan Haah, and Liang Fu, Fracton topological order, generalized lattice gauge theory, and duality, *Phys. Rev. B* **94**, 235157 (2016).
- [82] Bowen Shi and Yuan-Ming Lu, Deciphering the nonlocal entanglement entropy of fracton topological orders, *Phys. Rev. B* **97**, 144106 (2018).
- [83] Han Ma, A. T. Schmitz, S. A. Parameswaran, Michael Hermele, and Rahul M. Nandkishore, Topological entanglement entropy of fracton stabilizer codes, *Phys. Rev. B* **97**, 125101 (2018).
- [84] A. T. Schmitz, Han Ma, Rahul M. Nandkishore, and S. A. Parameswaran, Recoverable information and emergent conservation laws in fracton stabilizer codes, *Phys. Rev. B* **97**, 134426 (2018).
- [85] Huan He, Yunqin Zheng, B. Andrei Bernevig, and Nicolas Regnault, Entanglement entropy from tensor network states for stabilizer codes, *Phys. Rev. B* **97**, 125102 (2018).
- [86] Wilbur Shirley, Kevin Slagle, and Xie Chen, Universal entanglement signatures of foliated fracton phases, *SciPost Phys.* **6**, 015 (2019).
- [87] Jeongwan Haah, Bifurcation in entanglement renormalization group flow of a gapped spin model, *Phys. Rev. B* **89**, 075119 (2014).
- [88] Arpit Dua, Pratyush Sarkar, Dominic J. Williamson, and Meng Cheng, Bifurcating entanglement-renormalization group flows of fracton stabilizer models, *Phys. Rev. Res.* **2**, 033021 (2020).
- [89] Jonathan Francisco San Miguel, Arpit Dua, and Dominic J. Williamson, Bifurcating subsystem symmetric entanglement renormalization in two dimensions, *Phys. Rev. B* **103**, 035148 (2021).
- [90] Matthew B. Hastings and Jeongwan Haah, Dynamically generated logical qubits, *Quantum* **5**, 564 (2021).
- [91] Nicolas Regnault and Rahul Nandkishore, Floquet thermalization: Symmetries and random matrix ensembles, *Phys. Rev. B* **93**, 104203 (2016).
- [92] Daniel Ranard, Michael Walter, and Freek Witteveen, A converse to Lieb–Robinson bounds in one dimension using index theory, *Ann. Henri Poincaré* **23**, 3905 (2022).
- [93] Minh C. Tran, Andrew Y. Guo, Abhinav Deshpande, Andrew Lucas, and Alexey V. Gorshkov, Optimal state transfer and entanglement generation in power-law interacting systems, *Phys. Rev. X* **11**, 031016 (2021).
- [94] Andrew C. Potter and Takahiro Morimoto, Dynamically enriched topological orders in driven two-dimensional systems, *Phys. Rev. B* **95**, 155126 (2017).
- [95] Rahul Roy and Fenner Harper, Floquet topological phases with symmetry in all dimensions, *Phys. Rev. B* **95**, 195128 (2017).
- [96] Nathanan Tantivasadakarn and Ashvin Vishwanath, Symmetric finite-time preparation of cluster states via quantum pumps, *Phys. Rev. Lett.* **129**, 090501 (2022).
- [97] Ken Shiozaki, Adiabatic cycles of quantum spin systems, *Phys. Rev. B* **106**, 125108 (2022).
- [98] Maarten Van den Nest, Jeroen Dehaene, and Bart De Moor, Graphical description of the action of local Clifford transformations on graph states, *Phys. Rev. A* **69**, 022316 (2004).